Optimization of a GEM-Based Detector to Measure Tritium and Discriminate Against Other Radiation Types

by

Arvind Dhinakar

A thesis submitted to the
School of Graduate and Postdoctoral Studies in partial
fulfillment of the requirements for the degree of

Master of Applied Science in Nuclear Engineering

Faculty of Energy Systems and Nuclear Science

Ontario Tech University

Oshawa, Ontario, Canada

November 2019

THESIS EXAMINATION INFORMATION
Submitted by **Arvind Dhinakar**

Master of Applied Science in **Nuclear Engineering**

Thesis title: **Optimization of a GEM-Based Detector to Measure Tritium and Discriminate Against Other Radiation Types**

An oral defense of this thesis took place on November 22nd, 2019 in front of the following examining committee:

Examining Committee:

Chair of Examining Committee	Dr. Hossam Gabber
Research Supervisor	Dr. Anthony Waker
Examining Committee Member	Dr. Glenn Harvel
Examining Committee Member	Dr. Matthew Kaye
Thesis Examiner	Dr. Kirk Atkinson

The above committee determined that the thesis is acceptable in form and content and that a satisfactory knowledge of the field covered by the thesis was demonstrated by the candidate during an oral examination. A signed copy of the Certificate of Approval is available from the School of Graduate and Postdoctoral Studies.

ABSTRACT

Tritium poses a radioprotection issue, in the Canadian Nuclear industry due to the operation of its fleet of Canadian Deuterium Uranium (CANDU) heavy water reactors. Although it is a less penetrative radionuclide, tritium is shown to have a detrimental effect on the human body when ingested, inhaled or absorbed. GEM detectors have proven to be very useful in the detection of low energy ionizing radiation, with their ability to multiply electrons via avalanches and amplify the signal thereby increasing the ease of detection. This work aims to optimize the design of the collection plate of a GEM-based tritium monitor in order to discriminate between short and long-range beta particles and electrons. The THGEM gain was also investigated with experimental and computational modelling. Recommendations include modification of the collection plate and increasing the gain of the detector to improve the efficiency of tritium detection and discrimination against other radiation types.

Keywords: Nuclear; Tritium; Ion Chambers; Gas Electron Multiplier; Electron Avalanche

AUTHOR'S DECLARATION

I hereby declare that this thesis consists of original work of which I have authored. This is a true copy of the thesis, including any required final revisions, as accepted by my examiners.

I authorize the Ontario Tech University to lend this thesis to other institutions or individuals for the purpose of scholarly research. I further authorize Ontario Tech University to reproduce this thesis by photocopying or by other means, in total or in part, at the request of other institutions or individuals for the purpose of scholarly research. I understand that my thesis will be made electronically available to the public.

Arvind Dhinakar

STATEMENT OF CONTRIBUTIONS

I hereby certify that I am the sole author of this thesis and that no part of this thesis has been published or submitted for publication. I have used standard referencing practices to acknowledge ideas, research techniques, or other materials that belong to others. Furthermore, I hereby certify that I am the sole source of the creative works and/or inventive knowledge described in this thesis.

ACKNOWLEDGEMENTS

Firstly, I would like to thank Dr. Anthony Waker for his guidance, support and patience throughout the research. I would also like to thank Dr. Pedro Arce for assisting me with my Geant4/GAMOS issues. I am grateful to Dr. Heinrich Schindler and Dr. Rob Veenhof for going above and beyond in helping me with my Garfield++ coding problems. Lastly, I would like to thank my parents, my friends and colleagues for supporting me through difficult times and providing me the motivation I needed to finish the research project.

TABLE OF CONTENTS

LIST OF FIGURES

LIST OF TABLES

LIST OF ABBREVIATIONS AND SYMBOLS

DNAPL	Dense Non-Aqueous Phase Liquids
GEM	Gas Electron Multiplier
THGEM	Thick-Gas Electron Multiplier
CANDU	Canadian Deuterium Uranium
AECL	Atomic Energy Canada Limited
NRU	National Research Universal
MPC	Maximum Permissible Concentration
HTO	Tritiated Water
HT	Tritiated Gas
NRCC	National Research Council of Canada
NRC	Nuclear Regulatory Commission
OBT	Organically Bound Tritium
MCM	Monte Carlo Method
MC	Monte Carlo
GAMOS	Geant-4 based Architecture for Medicine Oriented Simulations
MWPC	Multi-Wire Proportional Counter
UNENE	University Network of Excellence in Nuclear Engineering
VRML	Virtual Reality Modelling Language

Chapter 1: Introduction

1.1 Tritium Generation in the nuclear industry

Nuclear waste is generated as part of many processes including the generation of power and the testing of nuclear weapons.[1] Amongst the various radionuclides emitted from nuclear waste, this thesis focuses on tritium. Tritium is a by-product of CANDU energy production and is generated by the interaction of neutrons from fission with the heavy water of the coolant and moderator via the following reaction: [2],[3]

$$^{2}_{1}H + n \rightarrow ^{3}_{1}H + \gamma + 6.26\ MeV; \qquad \text{(Equation 1.1)}$$

Once the tritium is generated in the primary coolant of the reactor, it is commonly found to seep through the high temperature metal seals and joints used in reactor containment leading to an increase in the discharge of tritium to the environment.[3] Controlling tritium exposure to the environment is directly related to controlling the moderator or coolant seepage. Schmutz et al.'s research showed that tritium generated in a CANDU reactor is of a different form (DTO) in comparison with other types of reactors (HT).[3] This form of tritium does not permeate through metals very well resulting in mitigation techniques involving coolant and moderator leak prevention.[3] Molten Salt reactors (MSRs) however tend to produce a more volatile version of the tritiated gas (HT) which will require a more specialized way of mitigation and containment.[3]

When Tritium decays to Helium it releases a beta particle given by the following equation:[3]

$$^{3}_{1}H \rightarrow ^{3}_{2}He + \beta^{-} + \bar{\nu} \qquad \text{(Equation 1.2)}$$

The resulting beta particles prove to be an internal hazard to the human body. Thus, the study of tritium production, detection, mitigation, and containment is of utmost concern.

In Canada, the Canadian Nuclear Safety Commission (CNSC) regulates tritium releases from CANDU nuclear reactors to the public and the environment.[4] Apart from certain standards set for the licences, the CNSC undertakes independent studies to mitigate tritium and its release to the environment.[4] However, tritium leaks are still seen in nuclear plants in Canada. In 1997, a heavy water leak at the Pickering-4 CANDU plant in Ontario, Canada released 50 GBq of tritium into lake Ontario which increased the tritium concentration to 100 times the background.[5] Similarly, in 1995, a valve failure at Bruce-5 resulted in a 25 tonne leak of radioactive heavy water.[5] Similar cases of tritium leaks can be seen in US based nuclear reactors as well. Tritium was found to be present in the groundwater at concentration levels above the drinking water standard in the 200-area of the Hanford site due to leaks from high level waste tanks.[6] A significant leak of tritium was discovered at the Exelon Braidwood facility in Illinois where more than six million gallons of tritiated cooling water were released to the environment over a nine year time by a faulty discharge pipe.[7] Thus, tritium subsurface contamination of nuclear sites pose a challenge as the contaminant source is difficult to locate and remediate.

Since tritium contamination is of utmost concern, researchers today are mainly focused on the understanding, predicting, and containing the subsurface contamination due to tritium. Tritium studies have shown that the average production of tritium in a CANDU reactor is 7.5e10 Bq per kg of deuterium per reactor.[4] Although tritium emission levels to the environment are strictly regulated, research studies have shown a greater incidence

of tritium levels in water bodies around nuclear plants.[4] In a study done by Sierra Club Canada, levels of tritium in drinking water in Ottawa reached 30 becquerels per litre on December 27, 2007, following the restart of NRU reactor at Chalk River.[8] Although the concentration of tritium in water was well below the regulatory limit of 7000 Bq/L, the radiation leaks must be controlled and contained to prevent a further increase of tritium in water. Moreover, when the NRU reactor was shut down following a power failure, there was a leak of tritiated water below the reactor vessel at the rate of 5kg/hour. [8]

With the increase in the number of leaks from nuclear sites, there is a possible increase in the subsurface concentration of tritium. Due to the adverse effects seen in the human body when ingested and inhaled, tritium continues to be a concern. Thus, the detection and discrimination of tritium from other nuclides is a priority for researches today. This thesis focuses on the detection of tritium using Gas Electron Multiplier based detectors, while providing an insight into discriminating and differentiation of tritium from other radionuclides in a mixed radiation field.

1.2 Tritium Characteristics

Tritium is the only radioactive isotope of hydrogen. It is considered to be the most important radionuclide released to the environment during the normal functioning of CANDU reactors since they use heavy water as a coolant and moderator.[4] Tritium has a mass number of 3 with a half-life of 12.32 years. Tritium decays to ^{3}He by emission of low-energy beta radiation with an average energy of 5.68 keV and a maximum value of 18.59 keV.[9] A tritium beta spectrum can be seen in Figure 1.1

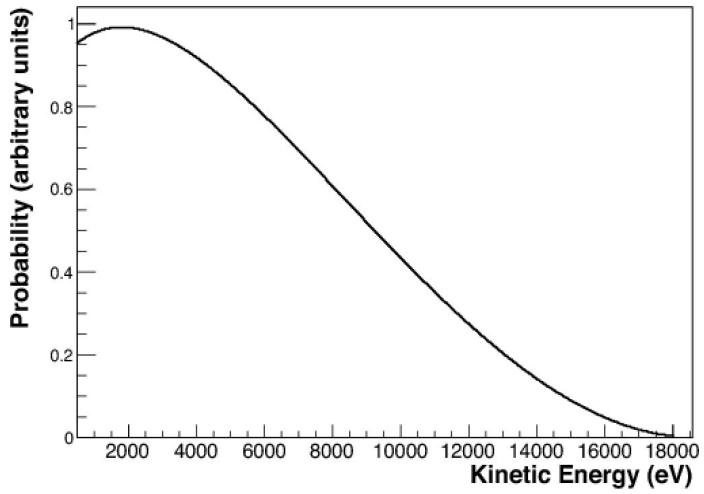

Figure 1.1: Tritium probability distribution for various energies.**[10]**

Tritium predominantly exists as HTO (tritiated water) and to a lesser extent as HT gas (hydrogen gas).[11] It is a weak beta emitter traveling a maximum distance of 4.5 mm in air and less than 600 μm in water, and does not represent an external radiation hazard.[11] Nevertheless, tritium represents a potential health hazard when inhaled, ingested, and absorbed by the human body.[11]

1.3 Biological effects of tritium

Two general factors must be considered while evaluating potential doses received from contact with tritium contaminated surfaces *i.e.,* exposure pathway and the physical/chemical form of tritium.[12] There are various pathways the human body can be exposed to tritium. These include external radiation, inhalation, ingestion, and absorption.[12] Since tritium has an average energy of 5.68 keV, and a maximum range of 6 μm in skin, thus skin penetration can be ruled out as an external radiation hazard. Tritium can exist as tritiated gas (HT) when exposed to air and tritiated water (HTO) when exposed to ground water bodies or water vapour in the air. Tritiated gas (HT) is formed when a

tritium atom replaces a hydrogen atom to form a tritium-hydrogen bond.[13] HT is an invisible, odourless gas chemically identical to hydrogen gas. HT is relatively inert in biological systems and has a very low uptake into body fluids and tissues.[13] When the human body is exposed internally via ingestion and absorption, tritium interacts with organic molecules and tissue to form OBT (organically Bound Tritium).[13] OBT can become incorporated into various compounds such as amino acids, sugars, and structural materials such as collagen.

When inhaled, tritium predominantly is found in the form of HTO and uniformly distributed in the body.[12] Research has shown that the half-life of HTO in the body is 10 days in comparison to organic tritium(OBT) which has a half-life of 40 days. [13] However, the damage done by HTO and organically ingested tritium is more or less similar at the DNA level.[12] Transmutation of tritium to helium is known to cause DNA damage resulting in DNA single strand breaks and interstrand cross links.[12] In a study performed by Torok *et.al.,* and Dobson *et.al*., tritiated water was found to be associated with a significant decrease in brain and genital organ weight in mice and also can lead to an irreversible loss of female germ cells in monkeys even at lesser concentrations.[14]

In a study by Laskey *et al*., rats were maintained on activities of 0.37–370 kBq HTO/mL of body water from initial conception of the first generation until delivery of the second generation progeny.[15] Although the first generation males showed a weight reduction in their genitalia, there was no impairment seen in their growth or reproductive ability. The second generation however experienced a greater reduction of brain weights and litter size.[15] In order to curb the long-term detrimental effects of tritium, there is a

need for the detection and control of tritium release into the environment and protection of the public and nuclear energy workers from exposure.

1.4 Tritium Monitoring

Consistent tritium monitoring and containment ensure that the tritium exposure is below the set regulatory limits.[6] Tritium monitoring ensures regulation standards are respected for the protection of the public and workers of nuclear sites. The CNSC is the governing body in Canada that monitors and regulates radiation released at or near CANDU nuclear power plants to the environment.[4] With the increase in the importance of tritium, the CNSC has addressed the lack of tritium research projects and has taken adequate initiatives to protect the public from tritium releases.[4] The Tritium Studies Project initiated by the CNSC in 2007, ensures proper funding and resources are available for tritium science and research to obtain better knowledge of tritium production in CANDU plants and how it can be contained or remediated.[4] Apart from Canada, other nuclear powers such as the US, the UK, and France have dedicated resources to the study of tritium and its containment. In its 2000 report on research needs in subsurface science, the Nuclear Regulatory Commission (NRC) of USA identified a lack of tritium remediation projects and has taken necessary steps to address its containment, stabilization, and monitoring.[1] An important component of the research needs, stated by the NRC, is the accurate monitoring of tritium and its contamination in the sub-surface.[1]

In 2000, Department of Energy, US expressed the research need for selective sensors appropriate for monitoring pure β emitters in water.[16] Thus, with the importance of tritium containment and monitoring, various organizations have initiated projects to improve tritium detection. In a mixed radiation field environment such as a nuclear power

plant, detection of tritium alone is very challenging as other radionuclides may affect data collection. Thus, a method of discriminating tritium from other radionuclides in a mixed field environment is also beneficial to the detection and containment of tritium. The Maximum Permissible Concentrations (MPC) for an individual exposed to tritiated water and tritium in air can be seen in Table 1. With the current dose assessment models, an exposure to 7000 Bq/L of tritiated water in a 'standard man' for average water consumption of 2 L per day will result in a committed effective dose of 0.1 mSv which is $1/10^{th}$ of the public dose limit of 1 mSv. Similarly, an exposure to $2*10^{10}$ Bq/m^3 of HT gas in a standard man at a breathing rate of 1.2 m^3 per hour for 2000 hours per year will result in a committed effective dose of 1 mSv Although the risk of tritium exposure to the human body is low, the dire consequences of exposure, provide enough motivation to effectively control and contain tritium release into the environment. While designing a tritium detector, factors such as the portability of the instrument and response time to the radionuclide are important design considerations. The various methods that have been used to detect tritium effectively are mentioned in the subsequent chapter.

Table 1.1: The Maximum Permissible Concentrations for airborne tritium and tritiated water for individuals in the public. **[4]**

Public Limit	HTO in Water	7000 Bq/L	0.1 mSv
Occupational Limits	DAC for HT in Air	$2* 10^{10}$ Bq/m^3	20 mSv

Chapter 2: Methods for Tritium Detection and Thesis Objectives

Tritium is a low energy beta emitter that is a common by-product of CANDU nuclear reactors. Since the beta particles emitted from the decay of tritium are low range, it does not pose an external hazard but when inhaled or ingested by the human body it fuses with organic molecules or exchanges with hydrogen in water and leads to a committed effective dose and a risk of cancer. Thus, the release of tritium into the environment must be strictly regulated. There have been a wide variety of tritium detectors that have been developed to efficiently detect tritium in various environments. The most important techniques are mentioned below.

2.1 Liquid Scintillation

Liquid scintillation is currently most direct and straightforward method of detecting tritium in water. The automated batch sampling system mentioned by Ting and Sullivan involves the use of liquid scintillators mixed with water samples to count tritium in a simplified scintillation counter.[17] The batch sample rate was calculated to be 10 batches per hour. However, failure in sample delivery due to selection of pump material and tubing decreased the accuracy in the results obtained.[18] This method was further modified by Huntzinger by using a cross-flow technique to obtain clean samples before mixing with the scintillation cocktail.[19]

A major problem associated with liquid scintillation is ensuring the proper mixing of the scintillation cocktail with the sample. This is heavily dependent on the mixing ratios of the scintillation cocktail and the use of metering systems to keep constant flow.[20]

2.2 Solid Scintillation

Due to the lower range exhibited by tritium, solid scintillators are seen to be less useful for the detection of tritium. However, plastic scintillators have shown some promising results in tritium detection. Plastic scintillators usually have the scintillator material coated or embedded on transparent beds optically coupled with photomultiplier tubes.[21] In a research study by Uda *et al.*, the plastic scintillators were seen to be less effective for tritium detection as the surface area of the scintillator exposed to the contaminated sample was not large enough to increase detection efficiency.[21] This result was further confirmed by Kumar and Waker, who found that the optimal scintillator thickness for efficient detection was 250 μm, but that sensitivity was insufficient for tritium detection in a mixed field environment.[22] A major advantage of solid scintillators is the reduction in waste produced compared to liquid scintillators.[21] However, while dealing with a low energy beta emitter such as tritium, various design considerations must be taken into account to improve detection efficiency.

2.3 Ionization Chambers

In case of tritium in air, ion chambers seem to be the ideal choice for detection. The earliest known tritium detector was the Kanne Chamber which was developed in the 1940s.[11] The gas to be investigated is drawn into an ion chamber where charge precipitation is forced by ion traps.[11] The resulting current due to electrons is measured using a picoammeter.[18] Marter and Patterson, concluded that although ionization-chambers are sensitive to air loading, external gamma and other radioactive gases, the problems associated with efficiency can be resolved by using an air filtering devices and

moisture traps.[23] From conventional air detection techniques, it is noted these instruments also lack the differentiation between long and short-range beta particles.[23]

A novel solution to the problem is the use of two chambers side by side with one of the chambers open to air to measure ambient radiation and tritium in air respectively as seen in Scintrex 209 and 309 models. This is referred to as gamma compensation.[24] The signals produced by the individual chambers are subtracted electronically to obtain the signal for tritium.[24]

2.4 Gas Ionization Counters

2.4.1 Proportional Counters

Proportional counters have been used for tritium detection due to their higher detection efficiency. A major advantage of proportional counters over ionization chambers is that ion chambers measure the total charge produced by the radiation in the form of a current, whereas, proportional counters detect individual radiation events.[20] Moreover, proportional counters unlike various other gas detectors have a higher electric field potential, which results in the acceleration of primary ionization electrons to form secondary electrons by colliding with the gas molecules.[25] However, a major disadvantage of proportional counters is the use of fragile electrodes exposed to the high electric fields to achieve higher gains needed for the detection of smaller ionization yields.[26] When the detector is operated consistently under these conditions, there is a possibility of a high ionizing event, which in turn increases the charge density. A charge density higher than the Raether limit, leads to the discharge of the device .[26] When faced with a similar problem Charpak *et al*., came up with the design of a multiple step avalanche chamber introducing the concept of pre-amplification.[27] A region of high electric field

between two meshes provide the primary ionization electrons a first boost of gain before transferring the charge to a second amplifying structure.[27] This basic principle used in the modern concept of Gas Electron Multipliers will be further described in the next section

2.4.2 Gas Electron Multipliers

Gas Electron Multipliers (GEMs) are used to amplify a charge drifting through the holes leading to higher gains. A conventional GEM design consists of two metal layers separated by a thin insulator etched with a matrix of holes.[28] There have been many developments in "Thick"-GEMS's (THGEM) in the last few years as it has 10 fold expanded dimensions compared to "Thin"-GEMs . It has shown to be more robust and have better resistance to discharge.[29] The THGEM foil consists of two 5 μm layers of copper that are separated by a 140 μm kapton foil.[30] Kapton used in THGEM foils is a plastic material exhibiting high thermal and mechanical stability along with a resistance to radiation damage which makes it a great material for use in THGEM devices.[31] Based on the necessity of the consumer, the copper foil is manufactured with high density chemically pierced pattern of holes usually between 50 to 100 biconical holes per mm^2.[30] A THGEM seen in Figure 2.2 designed by Orchard *et al.*, consists of 0.8 mm pitch with 0.4 mm hole diameter.[32] The thickness of the active region is 0.17 mm which is thicker than conventional thin-GEMS.

In principle, all GEM detectors have a system consisting of a drift region where all the gas ionizations take place. As seen in Figure 2.1, the bottom layer of the THGEM acts as the anode and the topmost layer in the detector acts as the cathode.

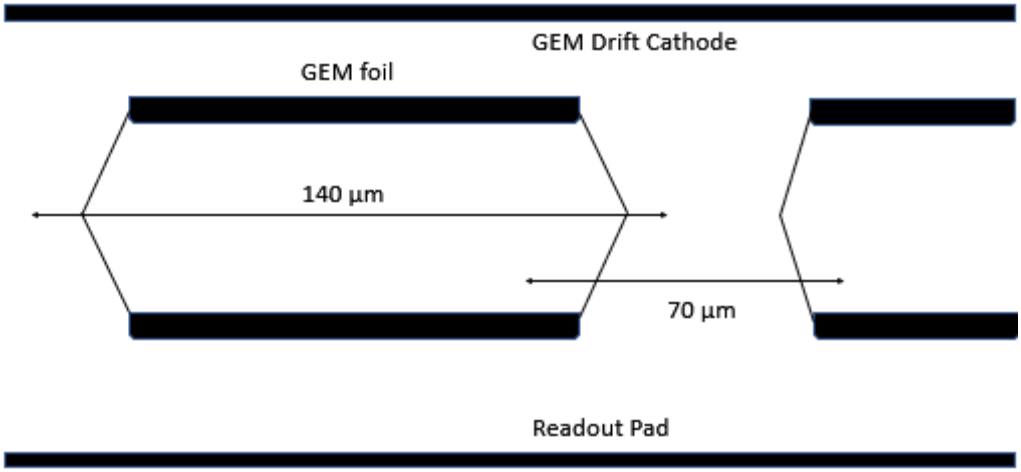

Figure 2.1 Schematic of a THGEM model used in the simulation

The electrons created by ionization move from cathode to the anode through the THGEM foil. The electric field created around the THGEM foil drives the electrons passing through them to undergo an electron avalanche. The avalanche is created by the electrons as they gain enough energy from the electric field between collisions to ionize on the next collision. The resulting multiplied electrons exit the THGEM and are driven through the induction region to the anode where they ultimately interact with the collection plate.[28] The THGEM hole diameter and shape have a direct influence on the performance and long-term stability of detector operation. Earlier studies have shown that to ensure higher gains the optimum hole diameter should be comparable to foil thickness.[33] In a study performed by Chechik *et al*., properties of Thick-GEMs and their functionality were actively investigated using gaseous detectors.[33] The effective gain in an Ar-CH_4 mixture could be increased by using multiple THGEMs in cascade.[33] The total cascade gain was found to be higher than the product of individual element gains due to the presence of a very high transfer field that penetrates the holes and modifies the multiplication factor.[33] Gas gains in THGEM detectors are low which corresponds to the stable operation thus

preventing discharge as discharge is directly proportional to the gain. This is seen to be a major disadvantage in THGEM detectors. However, the ability of a THGEM to provide higher gain using cascades and the value of discrimination on the basis of track length between various radiation types provides motivation for continued research.

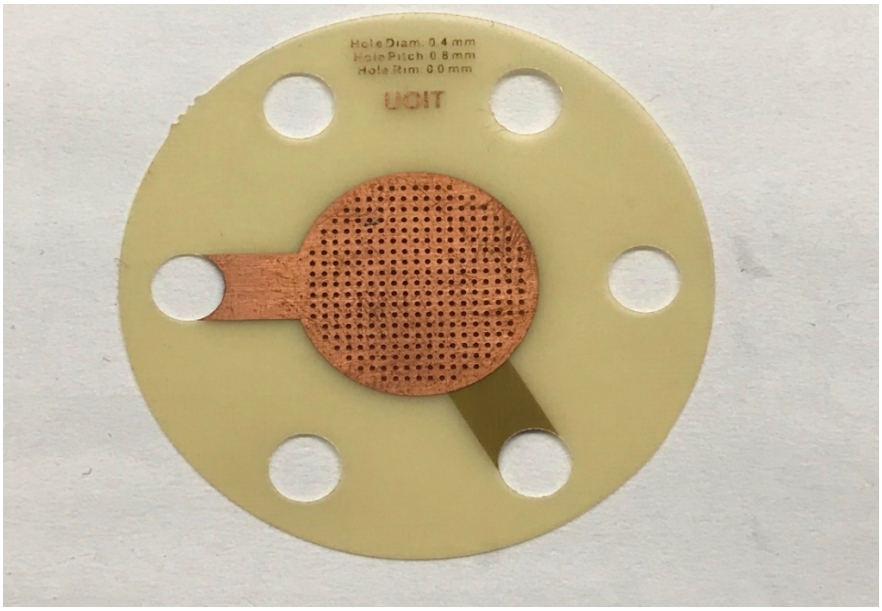

Figure 2.2 THGEM used in experimental determination of gain

2.5 Thesis Objectives

Tritium beta radiation does not penetrate the outer layer of the skin. Therefore, tritium only poses a health risk if inhaled, ingested or absorbed into the body through the skin. If the chemical form is HTO, it will not collect in any specific tissue or organ but will distribute itself uniformly throughout the body. If it is part of an organic molecule, it may be incorporated into specific molecules or tissues as OBT leading to an increased risk of cancer. Hence, there is a need for tritium detection and measurement. This can be achieved using THGEM based tritium detectors to amplify the signal obtained. Moreover, in a mixed field radiation scenario an ideal tritium monitor must be able to adequately discriminate tritium from other radiation types. This thesis will investigate tritium beta decay in a gas

and perform gain determination studies for THGEM detectors via both computational and experimental methods. Simulation studies will be reported that are used to make recommendations regarding the ideal collection pad size. Together, the two studies should provide the data for optimizing the design for a THGEM-detector for ease of tritium detection and discrimination against other radiation types.

2.6 Thesis Layout

This section describes a general layout of the chapters to come. A brief description of the chapter is provided along with the information it covers.

Chapter 3 will cover the background theory regarding the properties of beta particles and their interactions. Materials and methods used for both computational modelling and experimental setup will be discussed in detail. Software that will be discussed include Garfield++, Geant 4 and Elmer used for computational modelling. The experimental setup used and various settings to optimize the gain will also be discussed.

Chapter 4 focuses on the estimation of an ideal collection pad size for tritium beta radiation. A detailed description of simulation settings and the rationale for simulation will be provided followed by the results showing the tritium ionization cluster size formation in P-10 gas. Results from the simulation including the ideal collection pad size for tritium of the THGEM will be discussed.

Chapter 5 aims to focus on the experimental and computational gain of the THGEM. A comparative assessment of the simulation gain with a reference gain will be included. The dependence of simulation gain on THGEM voltage and penning transfer will be discussed along with the results obtained from both computational and experimental

methods. Furthermore, a comparative analysis will be performed for the results obtained in both simulation and experiment.

Chapter 6 will briefly summarize all the results from the above chapters and provide conclusions to improve detector design. Recommendations will be made regarding the collection pad size and increasing the gain of the THGEM. Finally, future development and use for the proposed detector will be addressed.

Chapter 3: Materials and Methods

3.1 Background Theory

This thesis focuses on tritium detection and discrimination using THGEM based devices. THGEM devices use gas-multiplication to increase the number of electrons thereby creating a bigger signal to study. In this thesis, both simulation and experimental methods are used to study THGEM devices, their gas gains and to make recommendations for the optimum collection diameter for tritium detection and discrimination.

3.1.1 Ionization by Beta Particles

Beta particles upon entering an absorbing media, interact simultaneously with many electrons. The electrons of the absorbing medium interact with the beta particle in the vicinity via the coulomb force.[30] Based on the proximity of the beta particle and the absorber atom, the energy of the beta may be sufficient either to cause excitation which raises the electron to a higher shell within the absorber atom or ionization where the electron is removed completely from the atom .[30] The beta particle as a result transfers some energy to the electron and its velocity decreases.

The ion pairs formed by the interacting beta particle usually have a natural tendency to recombine, but this recombination can be suppressed so the ion pairs can be used for the basis of detector response.[30] The relativistic expression for the maximum energy loss (Q_{max}) as a function of mass (M) for electrons can be given as:[34]

$$Q_{max} = \frac{2\gamma^2\beta^2mc^2}{1+\frac{2\gamma m}{M}+(\frac{m}{M})^2} \qquad \text{(Equation 3.1)}$$

Where, β represents the velocity of the particle with respect to the speed of light.

When, M = m for electrons and $\gamma = 1/\sqrt{1-\beta^2}$

$$Q_{max} = \frac{(\frac{1}{\sqrt{(1-\beta^2)}})^2 \beta^2 mc^2}{1+\frac{1}{\sqrt{(1-\beta^2)}}} \qquad \text{(Equation 3.2)}$$

Thus, simplifying the above equation to obtain:

$$Q_{max} = (\gamma - 1)mc^2 \qquad \text{(Equation 3.3)}$$

An incident charged particle can lose its energy entirely in a single head-on collision. However, since electrons colliding are identical to each other, it is impossible to tell which electron was incident.[34]

3.1.2 Drift Velocity and Diffusion of Electrons

When a uniform external electric field is applied to a gas, the electrostatic forces created as a result will tend to push the charges away from their point of origin. This net motion consists of a random thermal velocity and a concept called drift velocity of charged particles.[35] The drift velocity (v) of a charged particle can be defined as the mobility of a charged particle (μ) in an electric field of strength (E), inversely dependent on the pressure of the gas (p). This can be represented by the following equation:[35]

$$v = \frac{\mu E}{p} \qquad \text{(Equation 3.4)}$$

Where, μ represents the mobility of the gas, E the electric field strength and p the pressure of the gas.

The electrons under the influence of the electric field initially follow the path of the electric field line through their point of origin. However due to random diffusion, each electron generally takes a slightly different path from the other.

3.1.3 Electron multiplication in gases

As the electric fields are increased, the energies associated with the drifting electrons results in excitation and ionization of the gas molecules. During ionization, the incident electron produces an electron-ion pair where the newly created electrons can cause further ionizations. Thus, the electron density increases exponentially until they are collected at the anode. This process of gas multiplication in the form of a cascade is known as a Townsend avalanche.

The Townsend coefficient can be represented by equation 3.5.[35]

$$\frac{dn}{n} = \alpha dx \qquad \text{(Equation 3.5)}$$

where α represents the first Townsend coefficient of the gas and n represents the number of electrons.

The Townsend coefficient starts at 0 below an electric field threshold and increases with increasing electric field. The solution of α states that the number of electrons grows exponentially with increasing distance as the avalanche progresses. This can be given by the following equation:[35]

$$n\,(x) = n\,(0)\,e^{\alpha x} \qquad \text{(Equation 3.6)}$$

Where n (0) is the initial number of electrons and x is the distance.

3.2. Monte Carlo Simulation Methods

The Monte Carlo Method (MCM) was developed in the early 1940s as part of the atomic bomb program with applications in a wide array of fields including physics, finance, and system reliability.[36] It has enabled the use of statistical and mathematical models to simulate real-systems and then calculate the probability of event success.[36] The statistical or probability distribution must of course be known before MCM can be applied.

MCM is also well adapted to situations requiring an approximation of the stochastic events such as radiation interactions.[37] Monte Carlo algorithms tend to be simple, flexible, and scalable. MCM can be applied to systems ranging from the atomic scales to space science including black hole formation. This feature allows for both general and complex models to be studied easily on a computer.[37] In this thesis, Monte Carlo based simulation software such as Geant4 and Garfield++ were used to model ionization, electron drift, and gas-gain in a GEM-based detector arising from tritium beta decay.

3.2.1 Geant 4

The Geant4 Monte Carlo simulation toolkit offers a general-purpose platform for the simulation of particle-matter interactions.[38] It was developed by an international collaboration of physicists and software engineers. Since the software is open source, users can actively participate in forums and constantly provide updates to enhance its functionality. It includes a significant set of components for geometry description, particle definition, navigation and tracking, electromagnetic fields, and physics models. A schematic of the Geant4 system flow can be seen in Figure 3.1. The master program consists of the geometry and various user configuration settings that can be loaded at run time.[39] With each command, a process tree is set for the total number of threads or events. Each event has a local initialization, event loop and termination. After the stack of event threads are completed, they are merged as results with the master program and is seen as the output. In the context of this thesis, each event is one single electron. The state of each electron including properties such as energy, momentum, position, and direction are all initialized and run separately. The master program then combines all the results from each individual run to populate the result or output of the program. The toolkit is capable

of modeling a large variety of physical processes including electromagnetic, optical and hadronic interactions.[38] All physics models are selected based on the particle type and energy at run time.

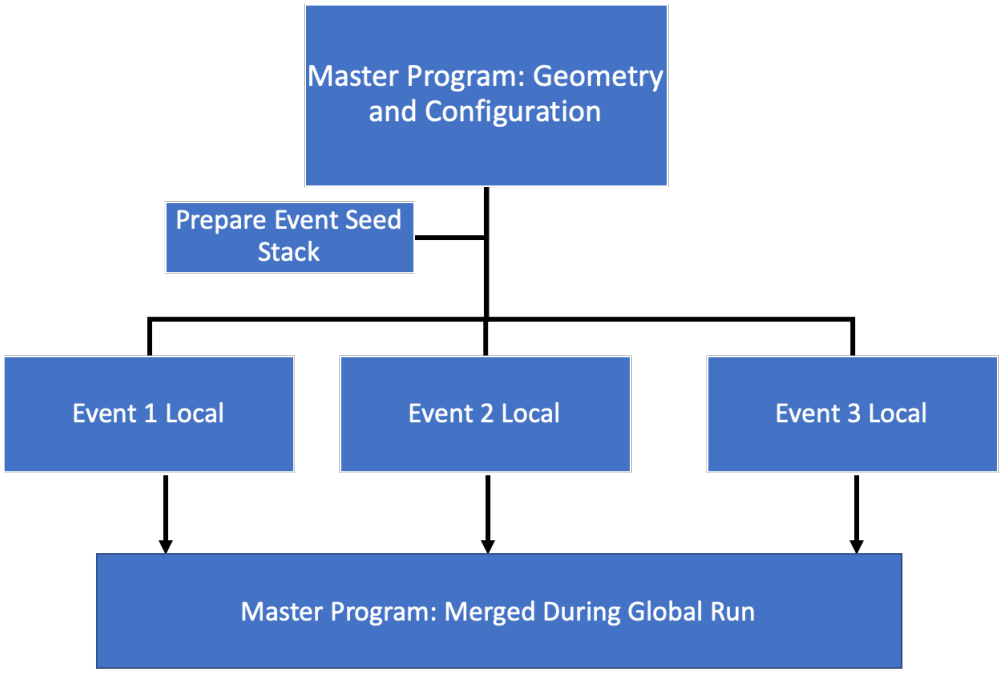

Figure 3.1 Program flowchart of Geant 4.

3.2.2 GAMOS

GAMOS also known as "Geant4-based Architecture for Medicine-Oriented Simulations is a Monte Carlo software that utilizes the program structure of Geant4 by making it simpler and more reliable for the end user.[40] The objective of GAMOS is to provide a software toolkit for the end user without having to know and learn C++ which is a base for Geant 4. To provide users with a greater flexibility, the GAMOS code is modular in nature which enables the main program to run without any predefined components.[40] The user sets in their components and they are loaded in at run time without a need to recompile the code.[39] An example GAMOS macro file to run a simulation is shown in

Appendix A. The GAMOS code can be classified into core and application modules. The core code is a set of classes that wrap the Geant4 kernel enabling the user to utilize its complete functionality through commands and plugins.[40] The application component uses the tools available in Geant4 and GAMOS core program or kernel, providing the user with custom simulation setups for a specific radiation or electromagnetic field. The GAMOS scripting language enables the user to specify desirable inputs without implementing any C++ code.[40] Most of the Geant4 user interface commands are extended to be used in GAMOS with the same scripting syntax. This enables the user to apply any Geant4 command to the GAMOS script. A schematic of the GAMOS program structure can be seen in Figure 3.2.

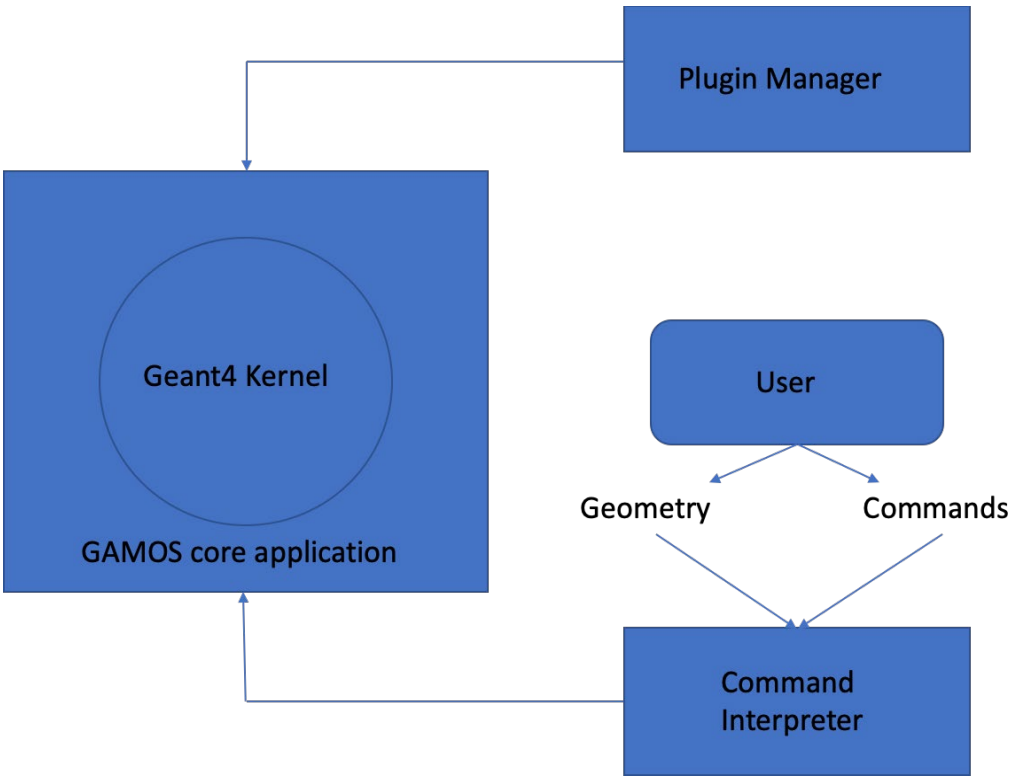

Figure 3.2 Program flowchart of Geant 4/GAMOS.

GAMOS has been based on the modular technology where each input is considered to be a module, since the beginning of its development to provide the framework with a relatively easy mechanism to cover all the possibilities offered by Geant4 even if the needed functionality was not foreseen by GAMOS developers[40] Without plug-ins or modules, adding a new feature in the framework would require a deep understanding of the framework structure and logic, and the framework code would have to be modified and recompiled.[40] Plug-ins enable customizing the functionality of an application without the aforementioned limitations. The user inputs such as geometry, nature of radiation, energy and direction are some examples of plug-ins. The user only has to provide his/her own code, and this code is "plugged into" the framework, which takes care of invoking the user component.[41] In this thesis, GAMOS was used to create a simple model with a predefined geometry and physics plugins to provide more information about tritium electron cloud formation resulting from a 5.68 keV average tritium beta particle.

3.2.3. Garfield++

Garfield++ is C++ based Monte Carlo simulation software developed at CERN in 1984 by Rob Veenhof and Heinrich Schindler as a successor to the fortran based Garfield. [29-41] This project was undertaken to help simulate various complex multipattern gaseous detectors. The Garfield++ toolkit consists of add-on codes including Heed and Magboltz to assist in tracking primary and secondary radiation. The program can also simulate the effect of electric field on radiation.[29]-[41]. Garfield++ utilizes the ROOT framework allowing easy visualization of electron and ion drift under the effect of electric fields.[42] An example of the Garfield++ code that simulates electron multiplication using a THGEM to show drift can be found in Appendix B.

The electric field for complex geometries like a THGEM cannot be calculated with Garfield++ alone. Subsidiary software with finite element solvers such as Elmer and Ansys and mesh generators such a Gmsh need to be used with Garfield++.[30] In this project, Garfield++ was used to simulate the working of an THGEM-detector with P-10 fill gas conditions for tritium beta particles. Data analysis was performed using simulated models of THGEMS with penning and non-penning effects to compare the gain achievable in P-10 gas.

3.3. Elmer and Gmsh

Garfield++ cannot be used solely for the calculation of more complex geometries of electric fields due to its lack of inbuilt functionality. Various other subsidiary software packages are used as plugins to Garfield++ to help with this issue. Gmsh is a three dimensional finite element generator that creates geometries and provides post processing functionality like meshing.[43] Its design goal is to provide a fast, light and user-friendly meshing tool with advanced visualization and user input capabilities. Input to the Gmsh modules are provided using ASCII text files or the graphical user interface.[43] All input files must be saved as a ".geo" format which is written in Gmsh's own scripting language. It is an open source program that can be used freely and redistributed. The basic structure of Gmsh is built around four major components such as the geometry, mesh, solver, and post processing.[43] The geometry can be designed with the inbuilt CAD design tool or imported from any CAD based software package. Dimensional meshing is done in 1D, 2D and 3D using mesh algorithms all producing grids of finite elements [41]. Gmsh was used in this thesis to port in a CAD based geometry and create finite elements to be used in an electric field solver such as Elmer. Elmer is an open source multi-physics simulation

software that includes physical models and electromagnetism.[44] The electric field is solved by partial differential equations specifically the Finite Element Method.[44]Using scripts, Garfield++ can be connected to Elmer and Gmsh to provide geometry meshes and electric field calculations at the same time, while setting up the initial parameters. In this project, Elmer was used to calculate the electric field potentials of finite elements in the THGEM geometry after meshing and designing with Gmsh.

3.4 Simulation Process Summary

In order to investigate the gas-gain and optimal collection pad size for tritium decay the above Monte Carlo codes were used. The first step in this process was to create a simplistic geometry in Geant 4 and use the same fill as would be used in an actual GEM device to see how tritium decay and ionization patterns could be viewed. GAMOS was used to create the geometry with a wide enough world volume so the electrons do not escape into the void. A mono energetic electron source of 5.68 keV representative of a beta particle from tritium decay of average energy was placed in the center of the cube releasing electrons outward in random directions as seen in Figure 3.3.

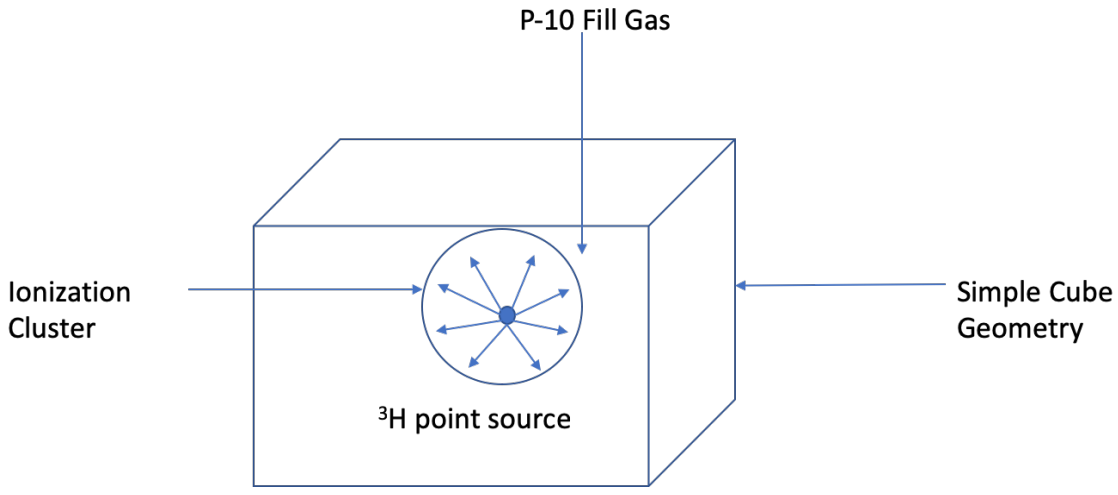

Figure 3.3 Schematic summarizing simulation parameters used in Geant 4

The result collected showed the average tritium ionization cloud size created. Since GAMOS could not show the secondary interactions and perform drift on these electrons Garfield++ was used. Garfield++ helps enables the calculation of the drift of the electrons and the collection radius on the collection plate. To test the efficacy of Garfield++, a simplistic geometry seen in Figure 3.4 was made and the electrons generated by the tritium beta were drifted down to the collection plate in a uniform electric field. A tentative collection diameter was noted by the highest intensity(electrons/mm^2) of electrons collected on the collection plate.

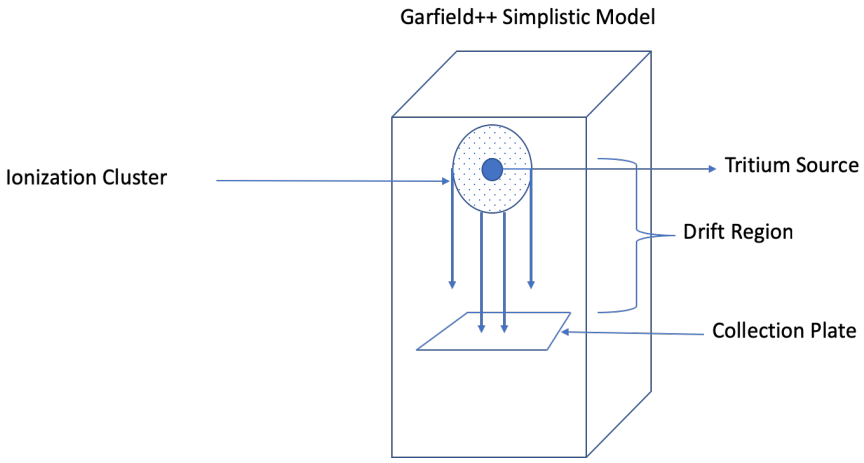

Figure 3.4 A simplistic model in Garfield++ simulation the drift of ionized electrons to the collection pad.

In order to investigate how the collection diameter value changes with the use of a Gas Electron multiplier, a THGEM simulation in Garfield++ was programmed. Since Garfield++ is not capable of simulating the drift of electrons stand alone, various subsidiary software mentioned above such as Elmer and Gmsh were used The model of the THGEM cell was designed in CAD and ported to Gmsh a mesh generator in order to create finite

elements in the geometry which can be used to solve electrostatic problems such as electric potential and electric field. The meshed model was ported to the finite element solver called Elmer which helped set the appropriate hole, drift and induction fields to simulate the THGEM. The data files obtained as a result were ported into Garfield++ for the drift and gain simulation. Similarly, the fill gas cannot be simulated standalone with Garfield++. A program called Magboltz was used to obtain the ionization coefficients, gas properties and diffusion coefficients for P-10 gas which was in turn ported into Garfield++ for the final simulation. Considering all these parameters the final simulation in Garfield++ sets the initial position, direction and energy of the particles before simulating the avalanche. The final output is the number of electrons released after the avalanche showing the gain and the collection diameter for the particle of concern. This can be simplified by the flow chart shown in Figure 3.5.

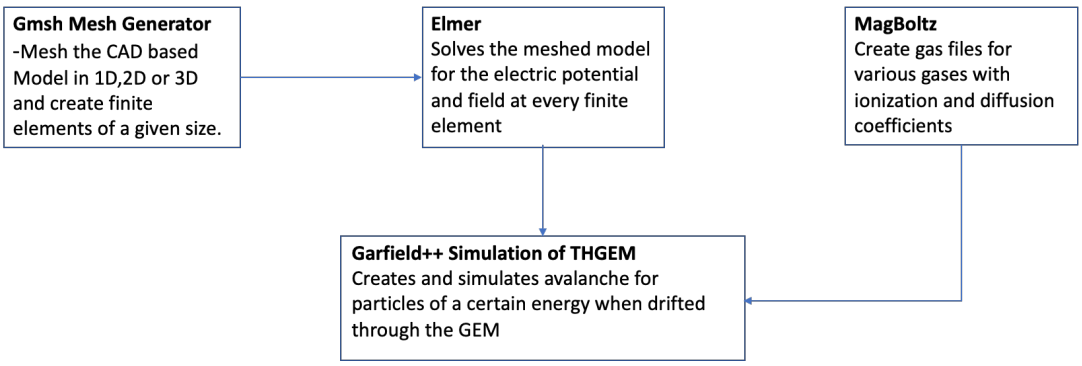

Figure 3.5 Schematic showing Garfield++ simulation process flow

3.5 Experimental Setup

The experiment was carried out in the setup seen in Figure 3.6. This setup was used to perform gain studies on a THGEM to compare with the simulation results. Initial gain

studies on the THGEM were performed using an Electron Mobility Spectrometer (EMS) designed and tested by Orchard *et.al*. The EMS consists of a brass and Teflon hollow cylinder, of length 92 mm and outer diameter 41 mm.[45] An Am-241 alpha source was used with a silicon surface barrier detector mounted opposite to each other. The surface barrier detector is used to detect the alpha particles emitted by the Am-241 source and crossing the ionization region of the device [45] The drift tube was filled with P-10 counting gas. A uniform electric field created using a voltage divider circuit in the EMS was used to drift the electrons to the collection region of the detector.

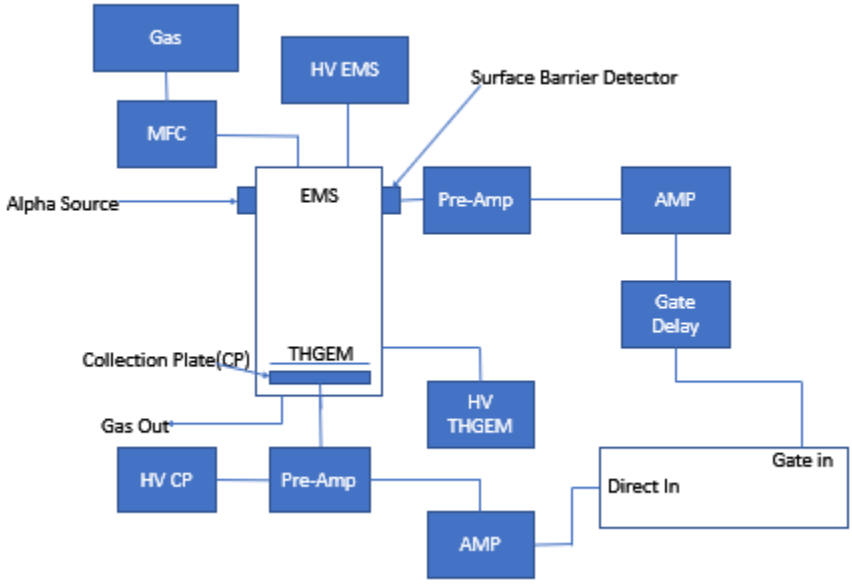

Figure 3.6 Schematic of experimental setup

The EMS device uses an anode wire in its design. The anode wire design was modified to incorporate a Thick GEM and a collection read out pad as seen in Figure 3.7.[32] The THGEM is a flat disc with a diameter of 41 mm composed of 0.12 mm thick insulator.[32] The active region of the THGEM is centered on the flat disc with each side

coated with copper resulting in a total thickness of 0.17 mm. The THGEM has 293 active holes with a pitch of 800 μm. A schematic of the THGEM can be seen in Figure 3.7.[32] A voltage of -1600 V was applied to the EMS drift region allowing the electrons generated due to ionizing collisions with the P-10 gas molecules to drift to the THGEM. The THGEM voltage was increased, applying a strong electric field within each hole creating a favourable region for gas multiplication. The resulting signal obtained at the collection plate was amplified using a pre-amplifier and a main amplifier to enhance and shape the signal collected at the collection pad. A multichannel analyzer was used to collect a pulse height spectrum for various high voltage settings applied to the THGEM and to the collection plate. The data acquisition system was also connected to an oscilloscope with which all the signal produced could be viewed. The Multichannel analyser software was utilized to obtain pulse height distributions of the Am-241 source as seen in the experimental results section 4. A schematic of the experimental setup can be seen in Figure 3.6 In order to observe and calculate the gain behaviour of the THGEM, the THGEM voltage was increased and the amplifier gains and gate delays were applied to the experimental settings. The results obtained were used to estimate the gain of the THGEM to compare with the simulation results.

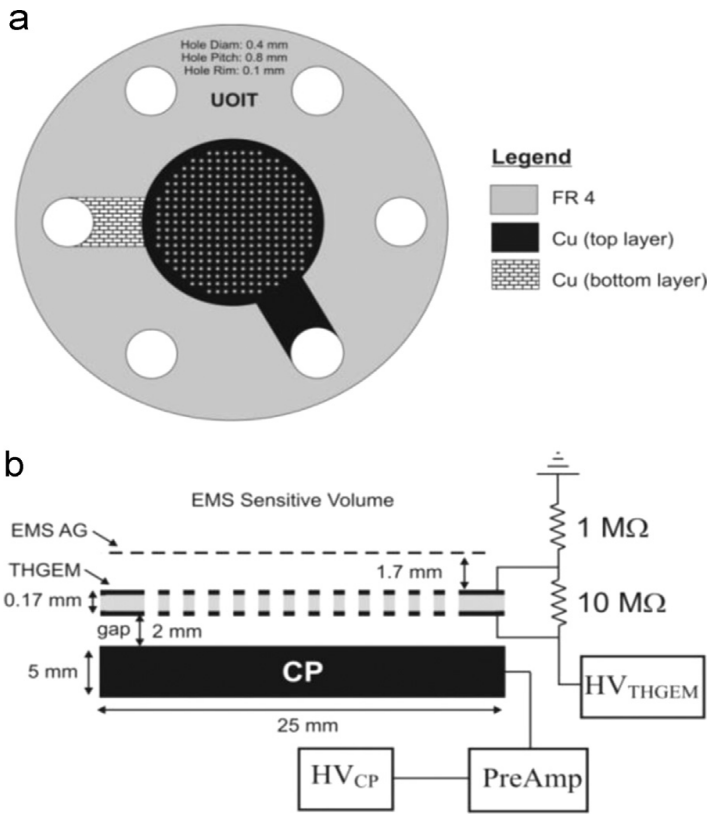

Figure 3.7 Schematic of the THGEM in the EMS design of Orchard *et. al*. **[32]**

Chapter 4: Determination of Ideal Collection Pad Size via Computer Simulation

Tritium monitoring has always been a challenge due to its decay products having low energy and low range in air. Current tritium monitors in the field use multiple ion chambers, avalanche photodiodes and various other modifications.[20] GEM based detectors have shown promising gains for the detection of various types of radiation including tritium. However, in a mixed field radiation scenario, an ideal GEM detector sensitive to tritium should also be able to adequately discrimination tritium from other types of radiation. Hence a method of tritium discrimination using collection pad size will be discussed below.

4.1 Rationale for determining the ideal collection pad size

Tritium detection and discrimination using gas electron multiplier is based on the measurement of the ionization cluster spatial information to determine the range of the emitting species.[20] THGEMs consist of thin self-supporting foil with copper cladding on both sides. When a beta particle is emitted in the sampling gas within the detector, it proceeds along a random path until it stops in the gas or meets one of the physical boundaries of the detector. The resultant ionization cloud is amplified by the GEM and detected by the readout pad. The THGEM acts as an intensifier that amplifies the signal within the defined drift region. The range of the beta particle will determine the number of pads triggered. A high energy beta or electron would trigger multiple readout pads whereas low energy betas such as tritium will only trigger one or two. Therefore, an ideal collection pad size for tritium can be established enabling the detector to detect tritium more efficiently. In conventional THGEM based tritium monitors the signal from tritium is much smaller than from equal concentrations of interfering radioactive gases.[46] The lack

of discrimination between tritium and other radioactive interferences frequently results in an overestimation of the tritium hazard. R. Surrette *et al.* [39] while trying to discriminate tritium from other interfering radiation injected tritium in the drift volume of a Double-GEM detector using the multiple readout pad design. The discrimination was done on the basis of track length with a higher energy particle having a longer track triggering multiple pads when compared to tritium with a shorter track triggering one or two pads. Since tritium has a maximum range in air of approximately 6 mm compared to Kr with 195cm and Xe with 74 cm , it can be differentiated and discriminated from other nuclear events. [46]

As mentioned in Chapter 3, a variety of Monte Carlo simulation software were used for this thesis study. GAMOS was used initially to determine the cluster size for tritium in a very basic geometry with a P-10 fill gas. A major limitation to the GAMOS simulation model was the exclusion of secondary and tertiary ionizations that result from the primary electron track. Moreover, the electron cluster generated could not be drifted using an electric field. This prompted the use of Garfield++, a Monte Carlo code for the simulation of electron drift. The electric field maps were generated with Elmer after meshing the geometry with Gmsh to provide the electric field for the THGEM. The gas properties such as ionization and diffusion coefficients were obtained by using Magboltz. This chapter focuses on computational results aimed at building a THGEM based detector that can effectively detect and discriminate tritium.

4.2 General Principles and Settings and Geometry of the Simulation

For determining the ionization cluster size distribution in GAMOS, the initial world volume was set large enough to be able to view the geometry using a VRML viewer. The world volume encompasses the logical and physical volumes in accordance with Geant 4

geometry builds. The gas used was a P-10 fill gas at standard temperature and pressure. The inner simulation cube was designed as a GAMOS physical volume with a dimensions of 2 x 2 x 2 mm in order to view the tritium beta particles effectively. A point source of electrons of 5.68 keV representing the average beta energy of tritium was placed in the physical volume used in the simulation set at origin. The physical and logical volumes were placed inside the world volume at origin. Electrons emitted was set to a random direction originating from the point source to identify the tentative size of the ionization cloud.

In order to determine the optimum pad size for tritium, Garfield++ was used to drift electrons down a simplistic geometry to observe the collection diameter on the collection plate. This simulation was done with and without the THGEM in order to observe if the GEM affected the spread of the electrons after multiplication. The geometry was designed as a 5 x 5 x 2.5 cm cuboid filled with P-10 gas at STP. A uniform electric field of 274 V/cm was initially applied to the geometry with the THGEM voltage set at 850 V. The initial energy of the beta particles was set to 5.68 keV which is representative of the average energy of tritium. The drift length and the drift field of both the simulations were varied to observe their effect on the collection diameter.

The ideal settings of a THGEM detector will depend on the THGEM dimensions, drift and transfer fields, the THGEM voltage, gas pressure and temperature. In a study performed by Shalem *et al*., these properties were tested and simulated for a standard THGEM.[47] The variation in the results by changing these properties gave an idea of the settings to be used in an investigation of collection pad size. The THGEM specifically investigated in this thesis was modelled with a hole diameter of 400 μm which is considered standard in the field for good electron multiplication.[48]

4.3 Simulated Ionization Cluster Size Distribution in GAMOS and Garfield++

The ionization cluster size was approximated by using the data set of the longest electron track as seen in Figure 4.1. 50 events exhibiting the average energy of tritium betas were released in the geometry with the track length calculated by using the initial and final coordinates of each primary event. The length of the longest track was obtained by sorting the data on the basis of track length. This was chosen as the radius of the tentative ionization cluster for tritium with which a sphere of influence was drawn keeping its center at the point source. It was assumed that all tracks that originate from the point source along with secondary and tertiary ionizations were contained within the enclosed volume seen in Figure 4.1. The settings of this simulation were discussed in the previous section. The ionization cluster size formation can be seen in Figure 4.1 with a cluster diameter of 0.8 mm.

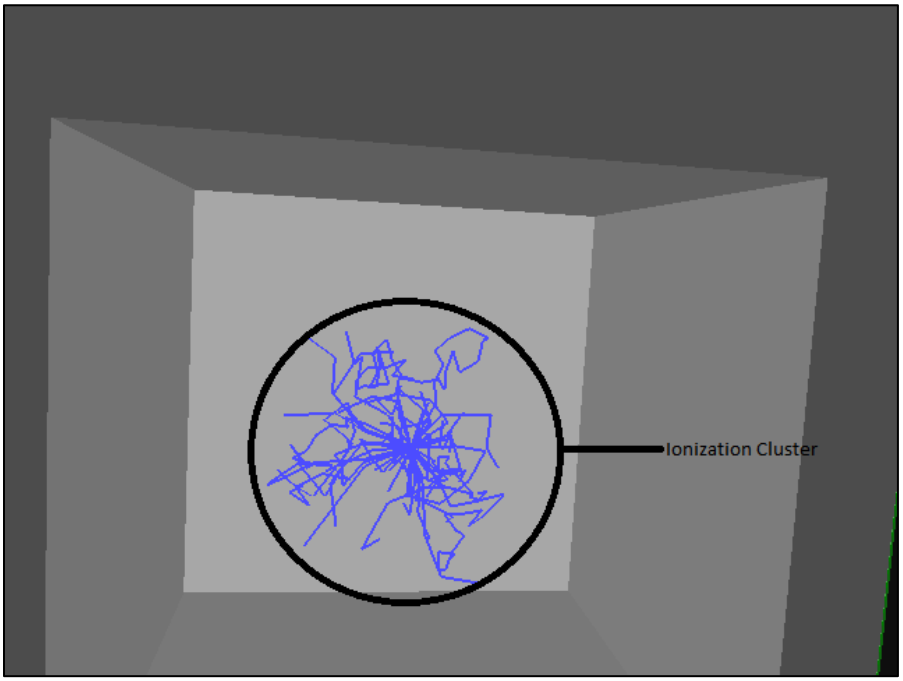

Figure 4.1 Simplistic cube model filled with P-10 gas depicting the ionization cluster size (zoomed-in image)

Using similar conditions, Garfield++ was used to simulate electron avalanche and collection without the use of the THGEM as seen in Figure 4.2. The base code was obtained from the Garfield++ website and modified to produce necessary results.[42] The ionization cluster was calculated by estimating the mean and standard deviation of the initial and final coordinates of the electrons created. The size of the ionization cluster was found to be 0.6 mm in diameter. Both the simulations in Garfield++ and GAMOS were run for 50 events. With minor variations taking into account the stochastic nature of radiation and the differences in the simulation codes, the cluster size of the ionization cloud seen in Garfield++ with a size of 0.6 mm was not far from the cluster size observed in GAMOS with 0.8 mm. The variation can be attributed to the cluster size definition in both the software. Due to the drawbacks of the GAMOS program, the ionization cluster radius was chosen as the length of the longest electron track with respect to the centre with which the ionization cluster diameter was calculated. Whereas in Garfield++ the ionization cluster diameter was computed as the spatial distribution of electrons in a certain area using the mean and standard deviation of the electron coordinates. These simulations were performed in order to observe deviation between ionization cluster formation in GAMOS and Garfield++ and to see the effect of drift of these electrons to the collection plate with and without the use of a THGEM.

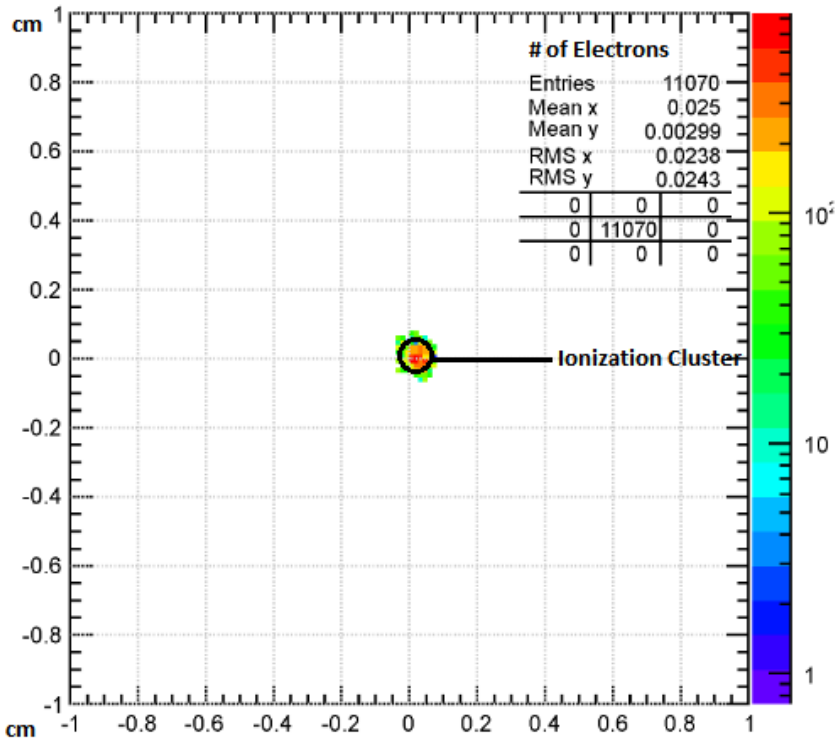

Figure 4.2 The ionization cluster size formation in Garfield++ for 50 tritium events at 5.68 keV average energy

Thus, the ionization cluster formation depends on the energy, type of radiation, and the properties of the fill gas. Tritium is a low energy beta particle and hence the cluster size is seen to be small. The electrons from this cluster are drifted to the THGEM using a uniform electric field to be multiplied using the avalanche process. The avalanche electrons exiting the THGEM will be driven to the collection pad through an induction gap using an induction field.

The thesis goals are achieved in a two-step process. The first step is to generate the ionization cluster due to tritium in GAMOS and Garfield++. The second step is to perform the drift simulation with and without a THGEM using Garfield++ to observe how the THGEM affects the spread on the collection plate. Due to the effects of the electric field on electron drift and charge spreading due to diffusion, the collection diameter is expected

to be larger than the ionization cluster generated. The spread of the electrons on the collection pad will provide information about the collection diameter with which a collection pad specific to tritium can be designed for discrimination against other radionuclides.

4.3.1 Collection pad size for tritium beta particles in Garfield++ without the THGEM

Mono energetic electrons having an average energy of 5.68 keV representative of a tritium beta distribution were released in a very simplistic detector model designed in Garfield++. The geometry was designed to be a solid cuboid of dimensions 5 x 5 x 2.5 cm. A uniform electric field of 274 V/cm was applied to the geometry filled with a P-10 counting gas. P-10 is a commonly used counting gas having a composition of 90% Ar and 10% CH4. P-10 gas is preferred as it is non-combustible and is a commonly used gas in low energy particle physics.[50] P-10 also shows a higher gas gain than Ar-CO2 which is another commonly used fill gas in nuclear physics.[50]

The ionization cloud created by a single primary event were drifted down a length of 0.1 cm and collected. Figure 4.3, shows an intensity plot of the electrons, colour coded with red being the highest intensity. The collection diameter was computed to be 1 mm, with the highest concentration of electrons shown in the red area as seen in Figure 4.3. Each individual point represents each electron collected at the collection point. For a single event where each event represents a tritium beta electron of 5.68 keV average energy, a total of 215 electrons were collected. The highest intensity (red) was chosen for the estimation of the ideal collection pad size as most of the energy deposition is seen in that

collection diameter in Figure 4.3. With this intensity plot, we can approximate the optimal pad size without the THGEM and investigate how consistent this is with a THGEM model.

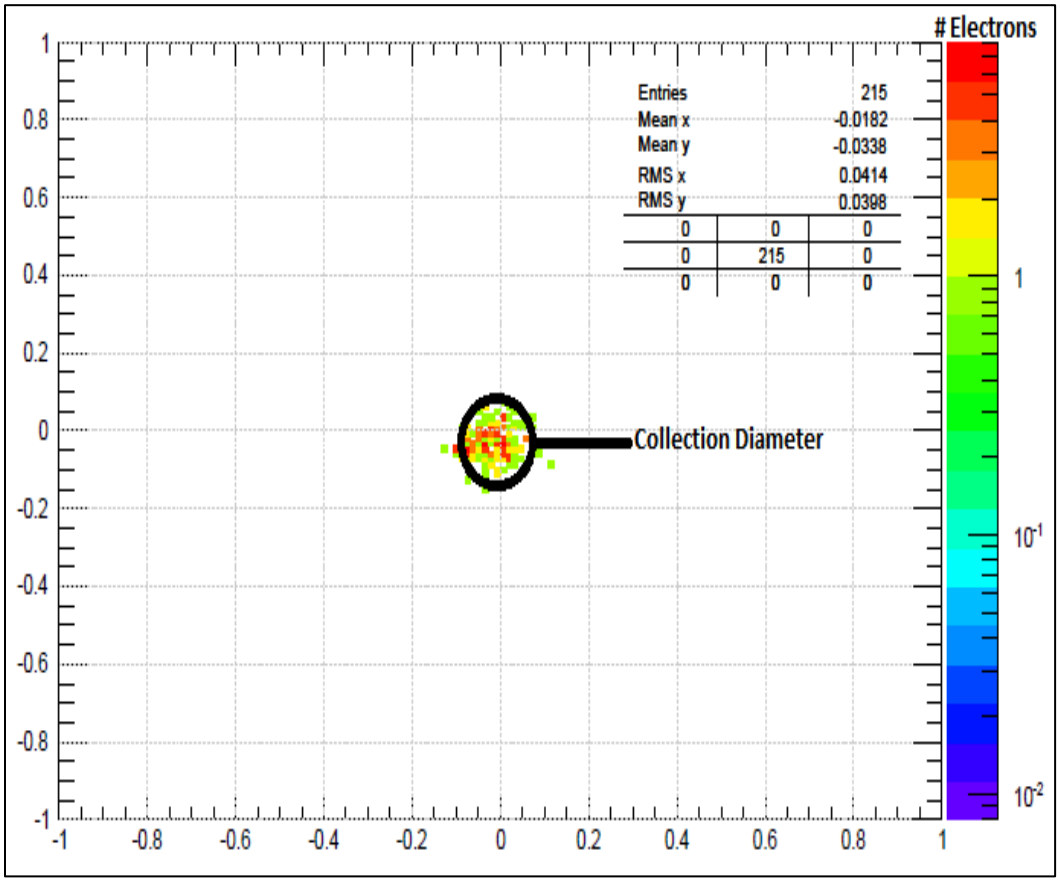

Figure 4.3 Intensity plot showing the collection radius without a THGEM device for 1 beta particle at 5.68 keV.

In order to investigate the effect of drift length on the collection diameter, the drift length of the simulation was modified from 0.5 cm to 5 cm. The results seen in Figure 4.4 suggests that by changing the drift length of the simulation, the cluster electrons take a longer time to reach the collection pad. This increases diffusion and increases the spread of the electrons on the collection pad.

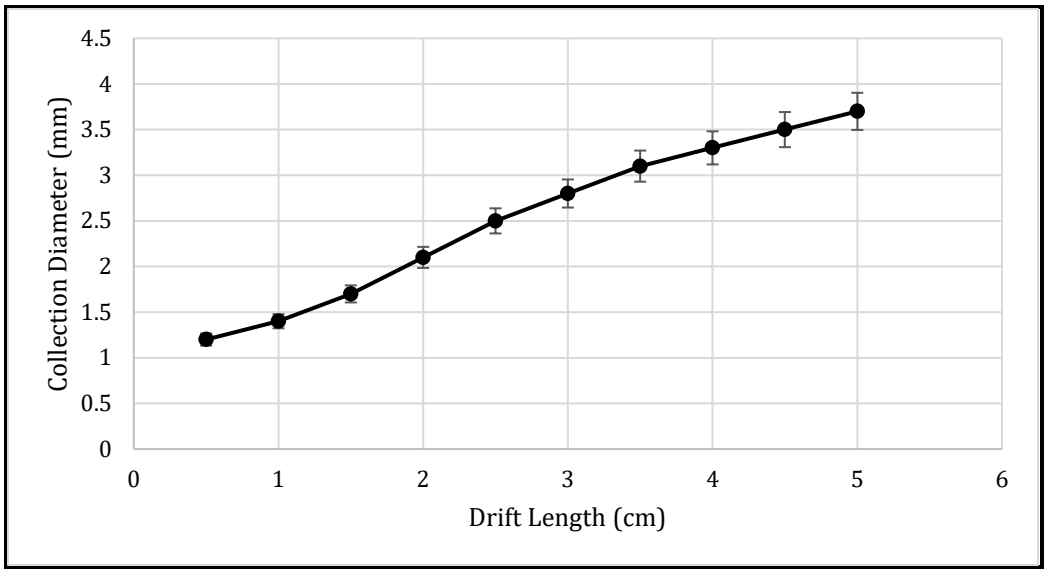

Figure 4.4 Drift length vs Collection diameter for 5.68 keV tritium beta particles without the THGEM.(Uncertainty discussed in Section 4.4)

To observe the dependence of the collection diameter on the drift electric field, the drift field was varied from 50-500 V/cm keeping other variables constant. The collection diameter, as seen in Figure 4.5, starts at a higher value at 50 V/cm and steadily drops since increasing the electric field increases the speed of electron collection and therefore decreases the diffusion time of electrons on their way to the collection pad thereby decreasing their spread. The overall decrease in collection diameter is around 10% over the electric field range simulated therefore varying the drift field within this range will not have a significant impact on the operation of a working detector with fixed collection pad size, however, there may be other advantages to having as fast a collection time as possible especially if electro-negative gases such as air are introduced into the detector along with tritium

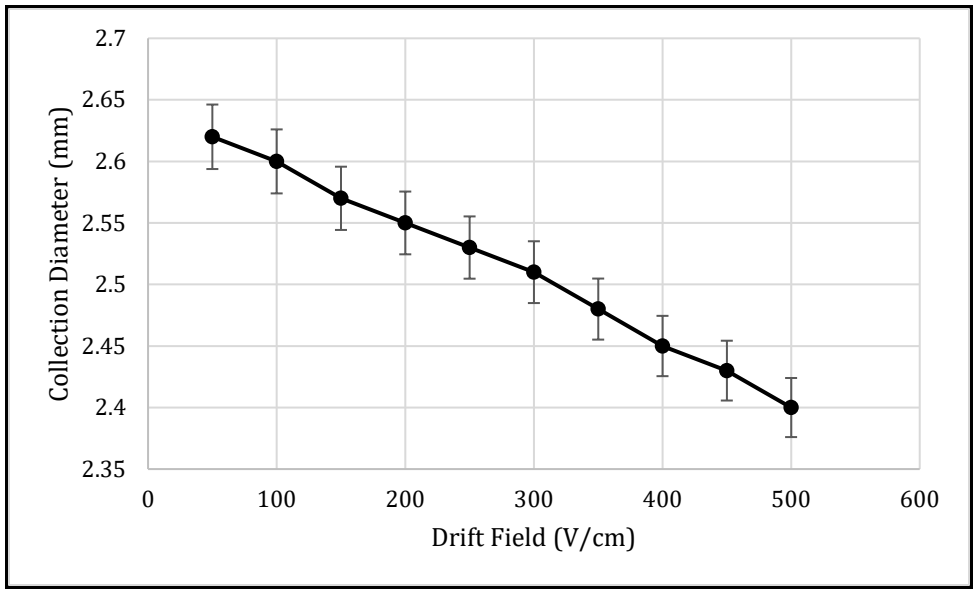

Figure 4.5 Electric field vs collection diameter for 5.68 keV tritium beta particles without the THGEM. (Uncertainty discussed in Section 4.4)

4.3.2 Collection pad size for tritium beta particles in Garfield++ with a THGEM

The Garfield++ simulation was designed with a THGEM to show how the electrons resulting from tritium beta particles were multiplied and the signal amplified for detection. The base code was obtained from the Garfield++ website and modified to produce necessary results.[42] This can be seen in Figure 4.6. A THGEM cell was chosen and designed with CAD. Meshing of the geometry was done in Gmsh to create finite elements and the electric field through the geometry was solved using the finite element solver Elmer. The gas properties including diffusion and ion mobility coefficients for P-10 gas were loaded into Garfield++ using the Magboltz program. The result shown in Figure 4.6 was simulated with a 5.68 keV beta particle released at 0.1 cm above the THGEM. The electrons released by ionization are drifted down by an electric field and multiplied by the GEM and collected at the readout pad with a 0.2 cm induction gap. The ideal collection diameter for tritium was estimated to be 2.2-2.5mm from the simulation. Comparing this

result with the previously obtained result for no THGEM of 1.0 mm, a variation can be observed. One of the factors contributing to this variance is the multiplication of electrons passing through the THGEM and the high transfer field in the induction region of the THGEM creating a wider spread.

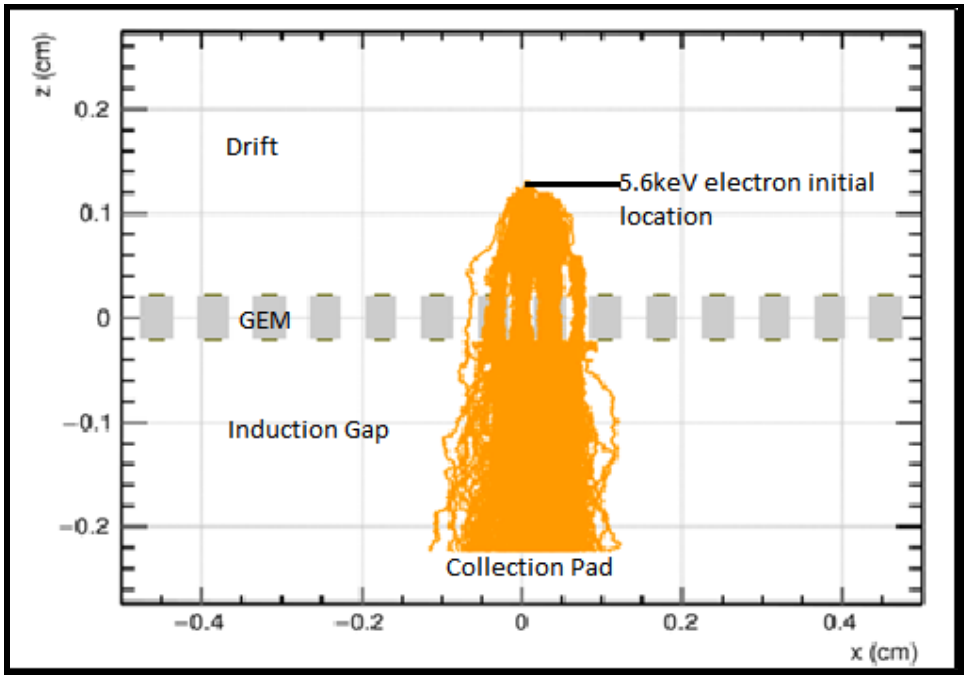

Figure 4.6 THGEM multiplication resulting from 5.68 keV beta particles.

Similar to the previous sub-section, the drift length of the THGEM model was varied from 0.5 to 5 cm to observe the effects on the collection diameter. As seen in Figure 4.7, the collection diameter increases with an increase in the drift length. As the electrons have a longer time to drift to the THGEM and increase chance of diffusion increases the collection diameter. Comparing Figures 4.7 and 4.4 for the same conditions we can observe similar trends but the differences in the magnitudes can be explained by the increase in collection diameter due to the presence of the THGEM.

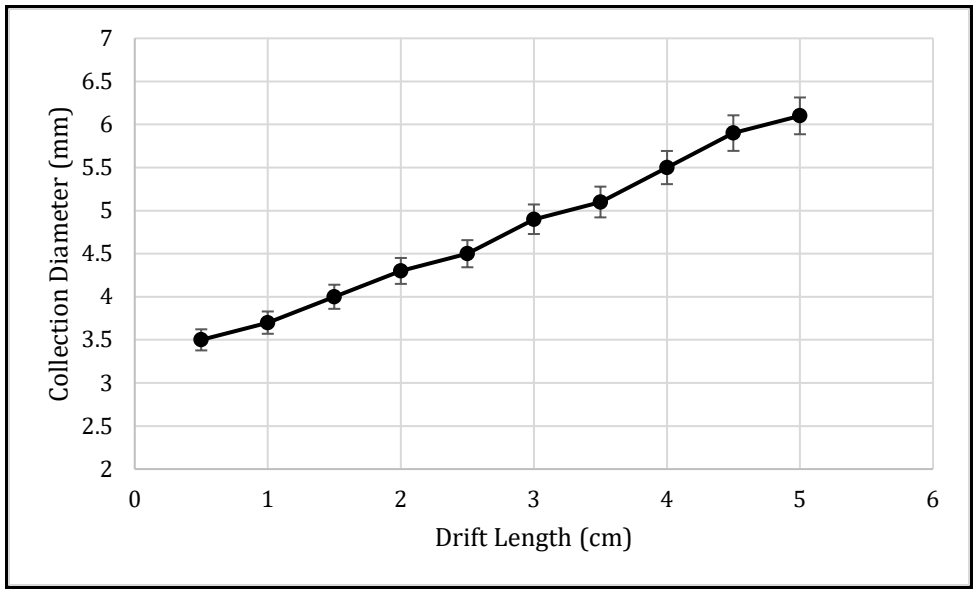

Figure 4.7 Drift length vs Collection diameter for 5.68 keV tritium beta particles with the THGEM. (Uncertainty discussed in Section 4.4)

Furthermore, the drift electric field of this simulation was varied from 50-500 V/cm to observe if the THGEM has any effect to the collection diameter. From Figure 4.8 it is evident that the trend seen was very similar to Figure 4.5. As the collection time of the electrons decreases, the electrons are less likely to diffuse and hence we see a reduction in the collection diameter. Comparing Figures 4.8 and 4.5 we can see similar trends but different magnitudes. This difference in the magnitude is attributed to the THGEM as it known to increase the collection diameter.

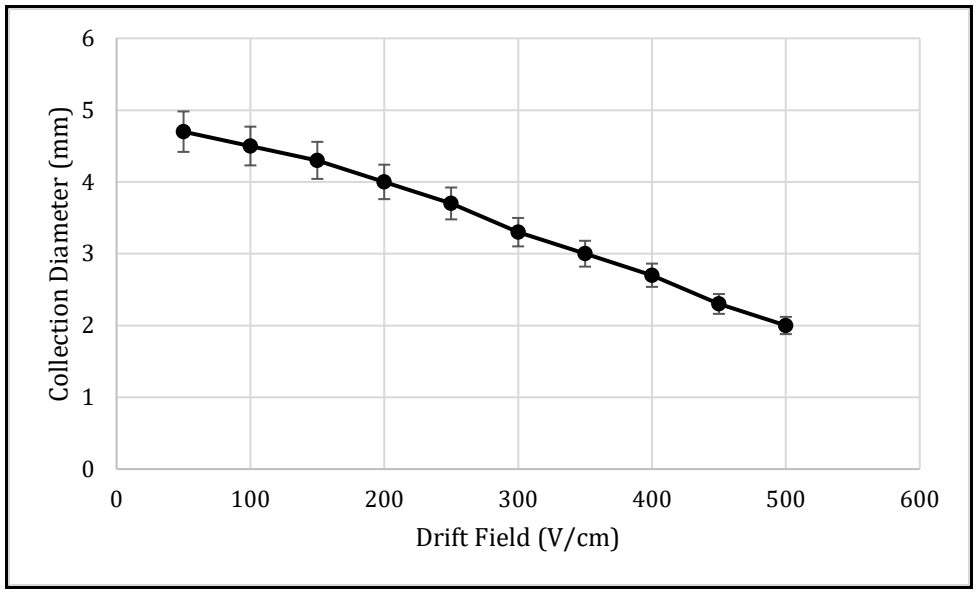

Figure 4.8 Electric field vs collection diameter for 5.68 keV tritium beta particles with the THGEM. (Uncertainty discussed in Section 4.4)

In order to estimate the ideal pad size for a drift length of 0.1 cm and a drift field of 274 V/cm the THGEM simulation was repeated 50 times to obtain a frequency distribution of the collection diameter recurring in the results. It was noted that this distribution was heavily dependent on the energy of the particle. The higher the energy of the particles released, the more the number of electrons produced and wider the collection diameter as a result. This will in turn shift the peak of the frequency distribution to the right. The results obtained can be seen in Figure 4.9. Some outlier collection radii were obtained while keeping the energy constant as seen in Figure 4.9, but this can be attributed to the stochastic nature of the avalanche process. Therefore, in the case of mixed radiation this ideal collection pad size can be effectively used to discriminate and detect tritium. This minimizes the over estimation of the signal in the case of mixed field radiation.

The ideal collection diameter only provides an estimate for the ideal pad size that needs to be designed when building a THGEM based multipattern gaseous detector capable of detecting tritium. However, since the source is a low energy beta emitter, gain studies

must be performed on the THGEM to make it viable for the detection. If the gain is seen to be on the lower end, then multiple THGEMs must be used in a cascade to exponentially multiply the gain. Gain studies with the THGEM are reported in Chapter 5.

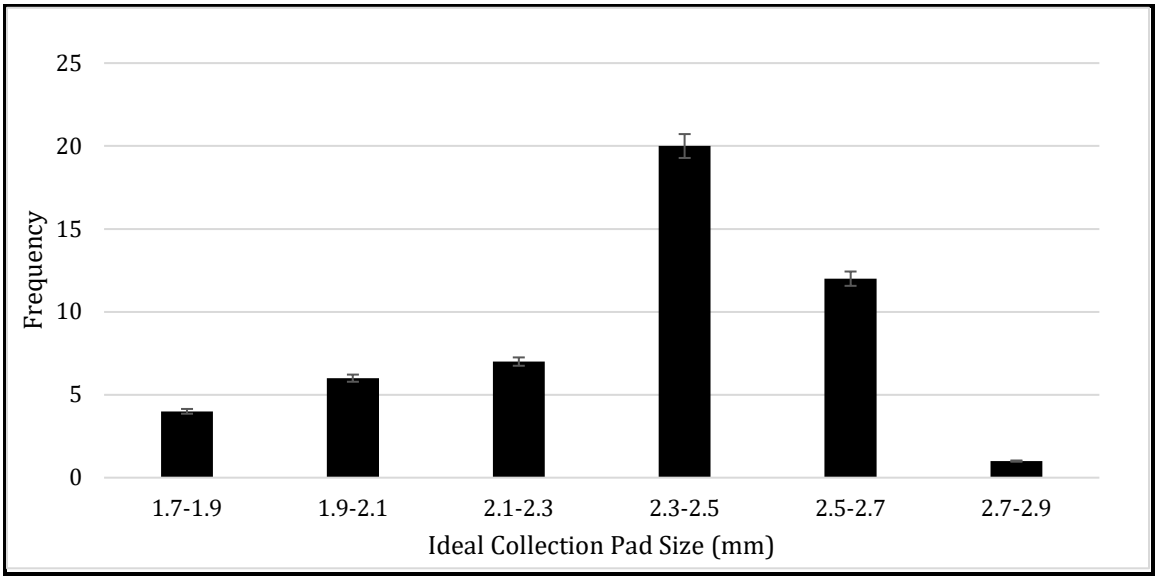

Figure 4.9 Frequency distribution of the THGEM simulation for 50 runs.

4.4 Calculation of Uncertainty in Collection pad size

The quantification of nuclear measurements involving non-linear components such as decay and radiation interaction contribute to the uncertainty in the measurement. For analytical measurements the total uncertainty can be calculated by computing the individual uncertainties of the parameters involved. However, in a computer simulation the uncertainty can be measured by running the simulation multiple times to obtain a range of results. Similarly, the simulation for the collection pad size was run 50 times and a frequency distribution of the pad size was obtained as seen in Figure 4.9. In Figure 4.9, the distribution is non gaussian in nature with the left tail longer than the right. Moreover, 38 out of a possible 50 values of collection pad size lie between 2.1 to 2.7 mm. This accounts

for 76% of the frequency with the reminder being outliers. The uncertainty of the pad size (σ_m) can be calculated as:

$$Uncertanity(\sigma_m) = \frac{\sigma}{\sqrt{N}} \quad \text{(Equation 4.1)}$$

Where, σ is the mean of the sample distribution and N is sample size.

Applying Equation 4.1 to this distribution, the uncertainty can be calculated as

11%

Chapter 5 Computation and Simulation of THGEM gain

5.1 Simulation and estimation of the THGEM gain

From theoretical studies of THGEMs, the operation principle is very similar to that of a conventional GEM. An electric potential when applied between two electrodes creates a strong electric field that helps with electron multiplication by the process of gas avalanches. The simulation setup consisted of a THGEM with hole diameter of 140 μm and hole pitch of 800 μm. The gas properties of P-10 gas were used in the model of the experimental setup. Magboltz was used to port in the gas properties such as ionization and diffusion coefficients into Garfield++. A schematic of the program flow can be seen in Figure 3.5.

An important factor to consider in the simulation when dealing with gases like P-10, are the effects on penning transfer on the absolute gain of the GEM. Penning transfer is a gain enhancement technique by which the gain of a system can be increased by adding a gas with a low ionization potential to a gas with a high energy excited state. Collisions between them increase the production of electrons and directly affect the gain of the THGEM device. [51] The existence of Penning effects in the gas has other repercussions. The ionizations due to excited atoms can lead to the "Jesse Effect" which can reduce the W-value of the gas.[51] The presence of impurities in gas mixtures can give rise to these effects and alter the gain of the system.[51] Thus it necessary to consider the Penning coefficient for the gas mixtures used in the simulation.

The simulation was designed to ensure similarity with the experimental setup in terms of gas pressure and temperature. The drift and the induction electric field was set as 274 and 1500 V/cm respectively and solved using a finite element solver, Elmer. The initial

energy of the particle was set at 5.68 keV which is representative of the average energy of a tritium beta particle. The initial position of the particle was set on the X-Y plane and drifted down the Z axis to the THGEM multiplication region and collection on the read-out pad. The number of electrons that have been multiplied is seen as the simulation output. This simulation output can be used to calculate the gain as discussed below. The simulation was run multiple times and a frequency distribution of the average number of electrons collected was plotted. This can be seen in Figure 5.1. The results for 50 events at 5.68 keV show that the modal value of electrons seen after gas multiplication is equal to 455.

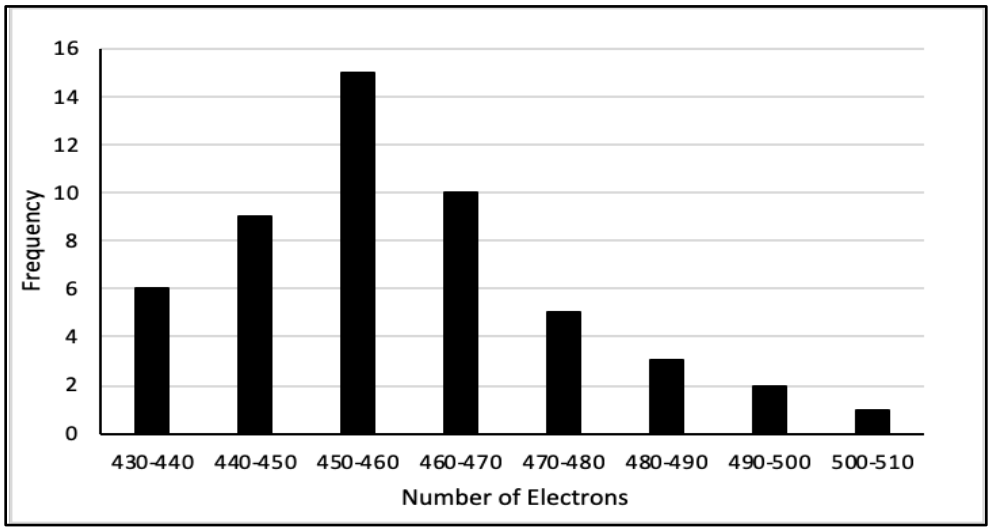

Figure 5.1 The frequency distribution of electrons collected for 50 events at 5.68 keV

This simulation was further modified to include an energy sampling technique which picks energies for the particle based on their probability of occurrence. The initial energy was set as to resemble a tritium energy spectrum. The tritium probability distribution was used with a random number generator to pick values of energies between defined bins according to their probability of occurrence. A single event in a program is representative of a single monoenergetic electron. For example, if 100 events are

initialized, the energy for each of these events will be chosen according to the probability of their occurrence representative of a tritium beta energy distribution seen in Figure 1.1.The code written to carry out the energy selection process was written in C++ and incorporated in to the Garfield++ model as an add-on as seen in Appendix B. The simulation was run 50 times and a frequency distribution of the number of electrons was obtained as seen in Figure 5.2.

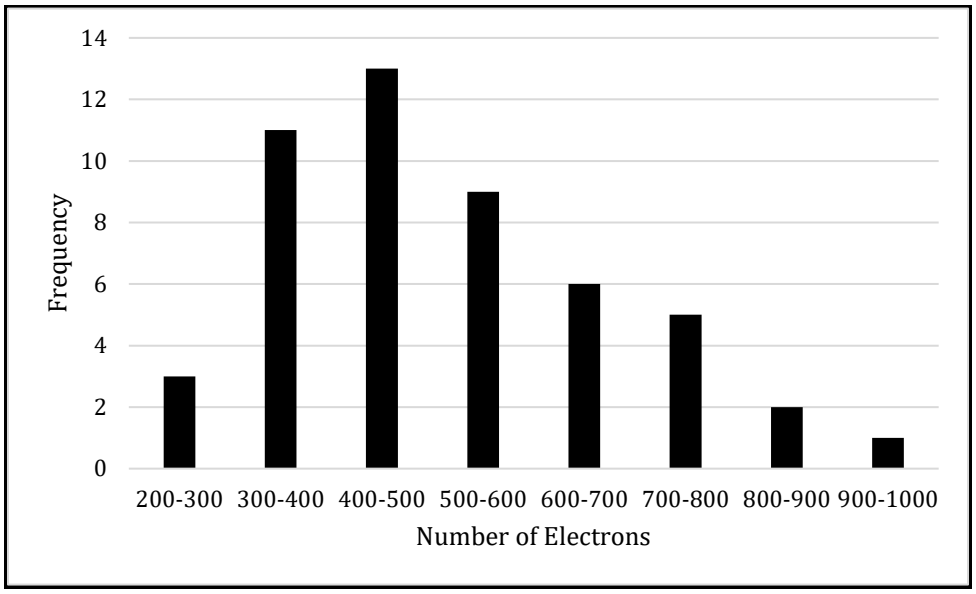

Figure 5.2 The frequency distribution of electrons collected for 50 events with energies following a tritium energy probability distribution.

The frequency plots of collected electrons after THGEM multiplication as seen in Figures 5.1 and 5.2, were converted to gain plots to observe the gain trends for both cases.

The gain of a THGEM detector can be calculated as follows:

$$\text{Simulation Gain } (G_s) = \frac{Electrons\ Collected}{Electrons\ Generated} \qquad \text{(Equation 5.1)}$$

Since the simulation results seen in Figures 5.1 and 5.2 provides the total number of electrons collected, the number of electrons generated can be calculated as follows:

$$\text{Electrons Generated} = \frac{Energy\ of\ the\ incident\ particle}{W_{gas}} \qquad \text{(Equation 5.2)}$$

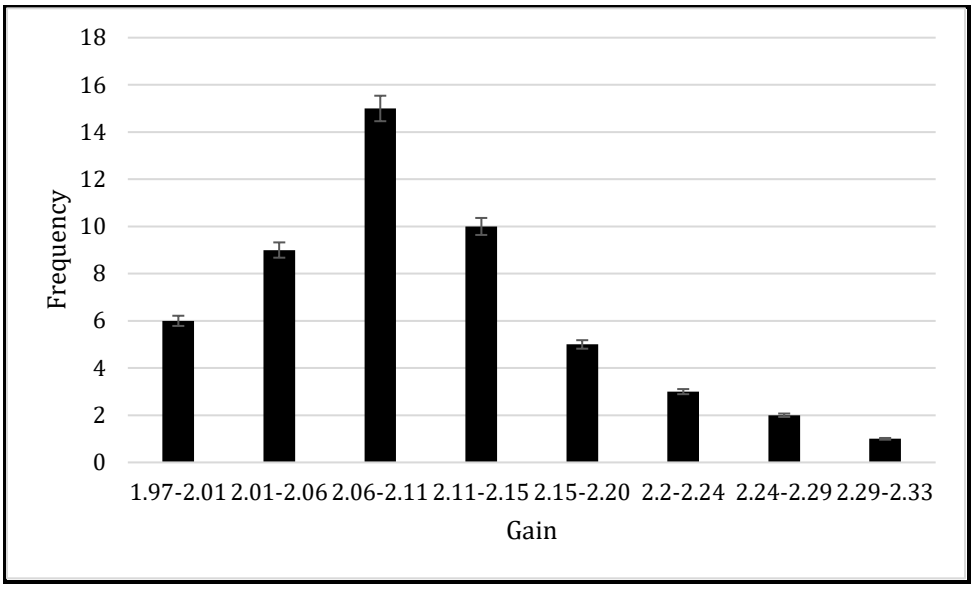

Figure 5.3 The gain plot for 50 events at 5.68 keV average tritium energy

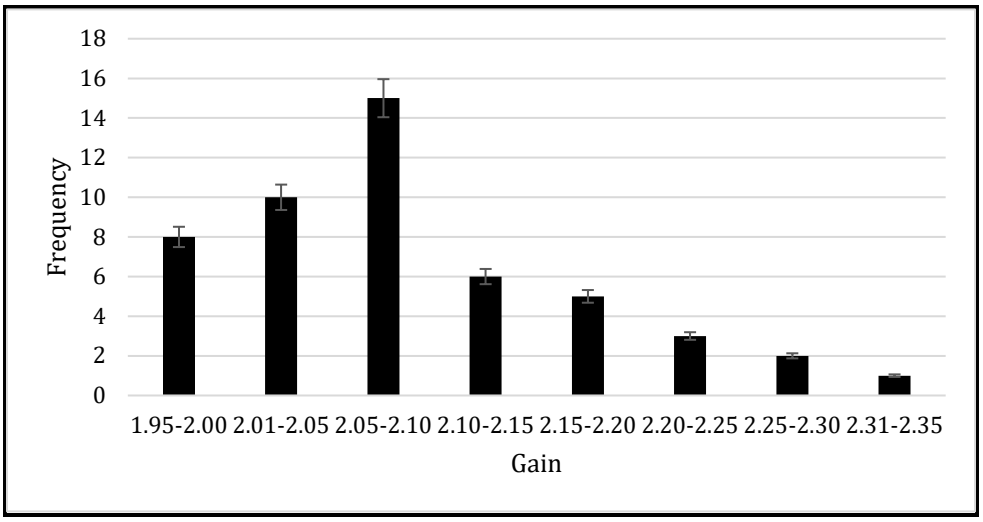

Figure 5.4 The gain plot for 50 events with energies following a tritium energy probability distribution.

From Figure 5.1, all incident particles have an average energy of 5.68 keV. The W value for P-10 gas under ideal conditions is measured to be 26 eV/ion pair. By substituting

these values into the equation, the average number of electrons generated is seen to be 220 for a single 5.68 keV beta particle. The modal number of electrons collected from over 50 runs as seen in Figure 5.1 is 455 and from Figure 5.2 is 450. Using Equation 5.1 the gain of the THGEM is calculated to be 2.1 for an average energy of 5.68 keV. Thus, using equation 5.1, the number of electrons collected seen in Figures 5.1 and 5.2 is converted to a gain plot seen in Figures 5.3 and 5.4 respectively. It can be observed that the gain trends seem to be very similar with the modal gain values as 2.08 for the 5.68 keV average energy and 2.07 for the tritium energy distribution. Given the uncertainties discussed below this difference in gain is insignificant which confirms that the gain of the THGEM doesn't not depend on the energy of the incident radiation.

This low gain value attained in both cases can be attributed to the design of the THGEM. In comparison to the conventional Thin-GEM design, the THGEM is a lot thicker having increased hole diameter and pitch. With an increase in the thickness the electric potential applied to the device will produce a weaker electric field. This will in turn affect the gas avalanche occurrence within the THGEM and decrease the number of electrons released compared to that of a conventional THGEM device. Moreover, changing the THGEM voltage and penning transfer coefficients of the gas affect the gain of the THGEM as seen below.

5.2 Dependence of Gain on Voltage

The voltage across the THGEM plays an important factor in determining the gain of the THGEM. By increasing the hole voltage, the electric field through the holes increases leading to an ultimate increase in the gain. The THGEM voltage was varied from 500V to 1200V in order to support this hypothesis. In order to test if the simulation code was

working as intended, Azevedo *et al.*'s GEM was simulated using the code used in this thesis. This was compared to the pre-simulated Azevedo *et al.* results.[52] The results seen in Figure 5.5 show great similarity between the simulated results and existing results of Azevedo *et al*. [52] proving that the code was working as intended.

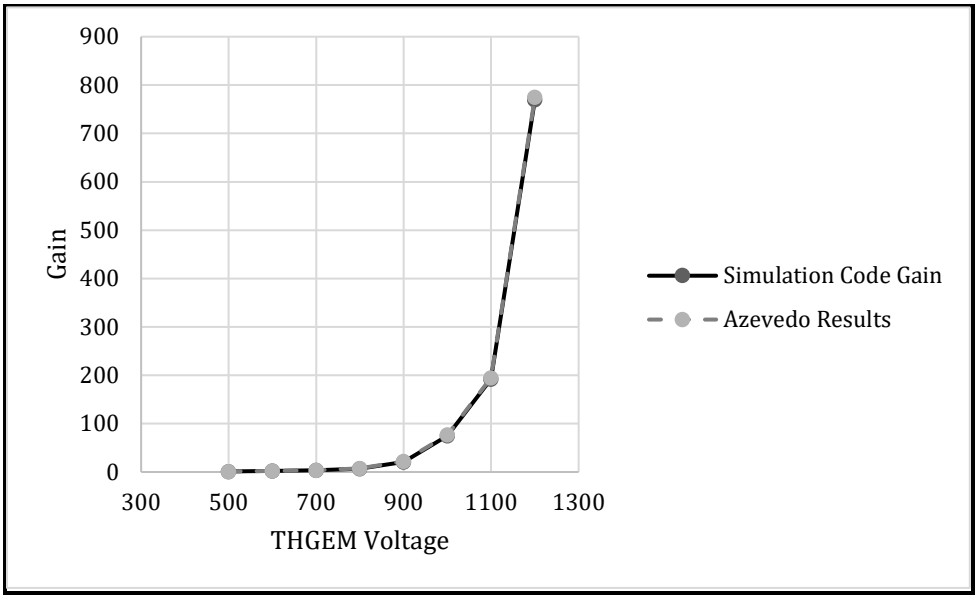

Figure 5.5 Comparing Azevedo *et al.*'s THGEM using the simulation code with the pre-simulated results obtained from the paper.[52]

The results shown in Figure 5.6 compares the dependence of THGEM voltage on the gain for different THGEM dimensions. For the sake of a reference, the THGEM design seen in the research study by Azevedo *et al*. [52] and the actual THGEM dimension used in experimental setup were considered. Both the THGEM designs were stimulated with the same conditions to test the versatility of the simulation. With an increase in the hole voltage larger avalanches are produced leading to greater multiplication rates and better gains. As observed in Figure 5.6. changing the voltage of the THGEM improved the gain from 2 to 100. When comparing the experimental GEM design to the results obtained by Azevedo et.al, [52] little deviation from ideal behaviour was observed. Their results coincide closely with the results obtained in this gain study proving that the dimensions of the THGEM

have little effect on the gain of the THGEM in this case. However, by changing the voltage of the THGEM, the gain increases. An increase in the voltage increases the electric filed through the holes of the THGEM which increases the size of avalanches and hence increases the gain.

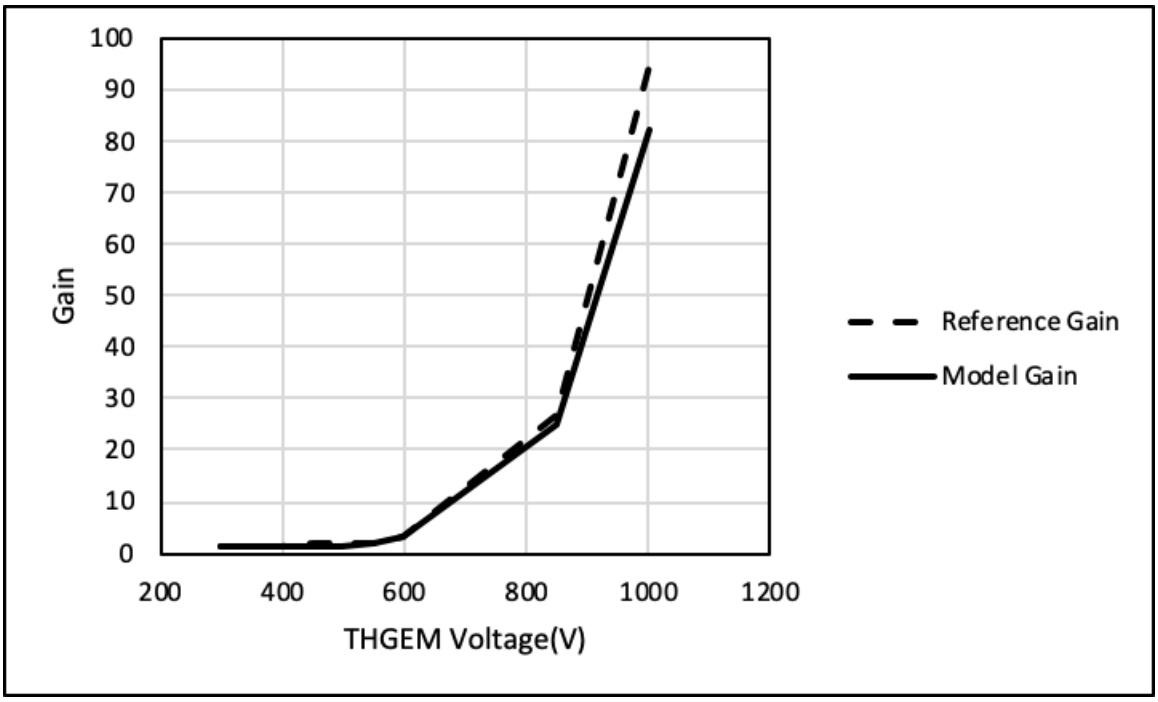

Figure 5.6 Comparison of simulation gain(our model) with results seen in Azevedo *et al.* **[52]** with increasing THGEM voltage.

5.3 Dependence of Gain on Penning transfer

While increasing the THGEM voltage provides a higher gain as discussed above, the Penning effect in the gas proves to be a very important factor in determining the absolute gain of a THGEM. In order to investigate the dependency on Penning effects, the THGEM voltage was modified under two conditions i.e. with and without Penning transfer. As mentioned previously, Penning transfer is a gain enhancement technique achieved by adding a gas with a low ionization potential to a gas with a high energy excited state. Collisions between the gas molecules, increase the production of electrons and directly

increase the gain of the THGEM device. A Penning transfer coefficient of 0.19 or 19% was used in this simulation for P-10 gas at STP. As seen in Figure 5.7, at low voltage ranges, the Penning effect is not very prominent as the electric field produced by the THGEM is not strong enough to drive the electrons to undergo multiplication. As the voltage of the THGEM is increased further, a drastic difference can be seen between Penning and Non-Penning gains. This can be attributed to the increase in the number of electrons produced due to the higher electric field creating further ionizations and thereby increasing the chance of Penning effects. Although the trends between Penning and Non-Penning gain seems to be similar, the magnitude of gain increase is drastically different. For example, in Figure 5.7, at 1200V, the Penning gain is at 700 while the Non-Penning gain is at 10.

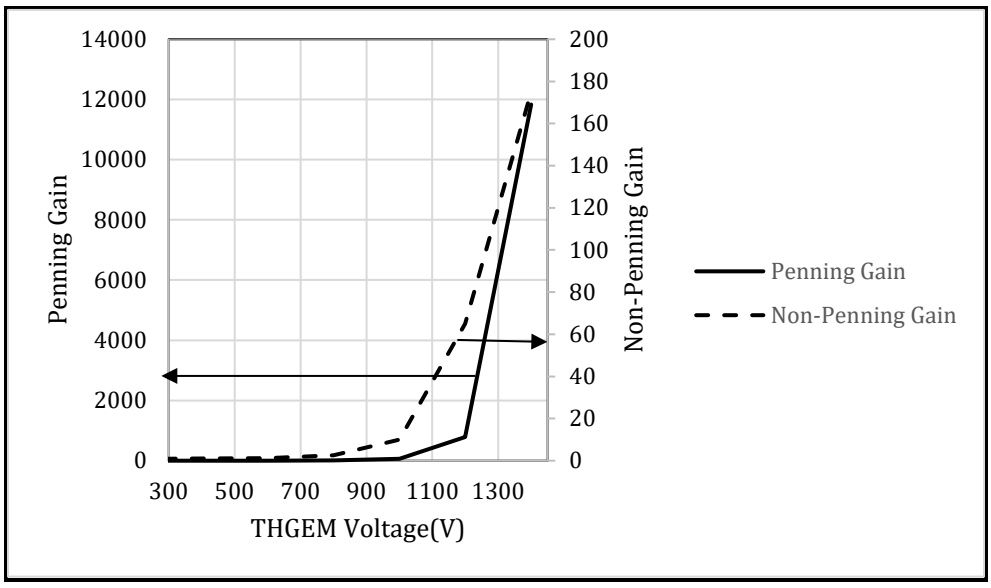

Figure 5.7 The effect of THGEM voltage on the gain with and without Penning transfer.

5.4 Experimental estimation of THGEM gain

The experimental setup mentioned in Chapter 3 was used to perform all the experimental work to compute measure the gain of the THGEM. Since, in principle, THGEM gain is not dependent on the source of radiation, as described earlier an alpha source is used to generate the initial electrons from the measurement of the absolute gain of the THGEM. The results from the measurement of the absolute gain of the THGEM were compared to the simulation gain obtained this chapter in order to make recommendations for a tritium detector design.

5.4.1 Determining the count rate for Am-241

As the apparatus described in Chapter 3 and used by Orchard *et al*. [32] has been partially dismantled, the first experiment involved measuring the alpha count rate as a function of gate delay to show that the experimental setup was again functional, and the results obtained were in accordance with Orchard *et al*.[32] The experimental setup started off with a THGEM voltage of 550 V with the main amplifier settings at 5 and 25 creating a total amplification of 125. The setup included a surface barrier detector that triggered on the alphas travelling straight from the source to the detector horizontally across the ionization region of the EMS. The amplified and shaped alpha signal was in turn connected to a gate delay generator that assisted in estimating the travel time of electrons flowing down the EMS in the original experiment of Orchard *et al*. [32], and also ensured that only the signals arising from alphas crossing the ionization region were measured. Both the signals arising from the collection plate of the THGEM and the gate-delay generator are connected to a Multi-channel analyzer such that the THGEM pulses resulting from non-scattered alpha particles were recorded. The experiment was performed by changing the

gate-delay settings and observing the resultant count-rate for the pulse-height spectrum recorded from the THGEM output. The results seen in Figure 5.8 show that the counts per second initially is low as the delay set does not match up with the transit time of electrons drifting down the EMS.

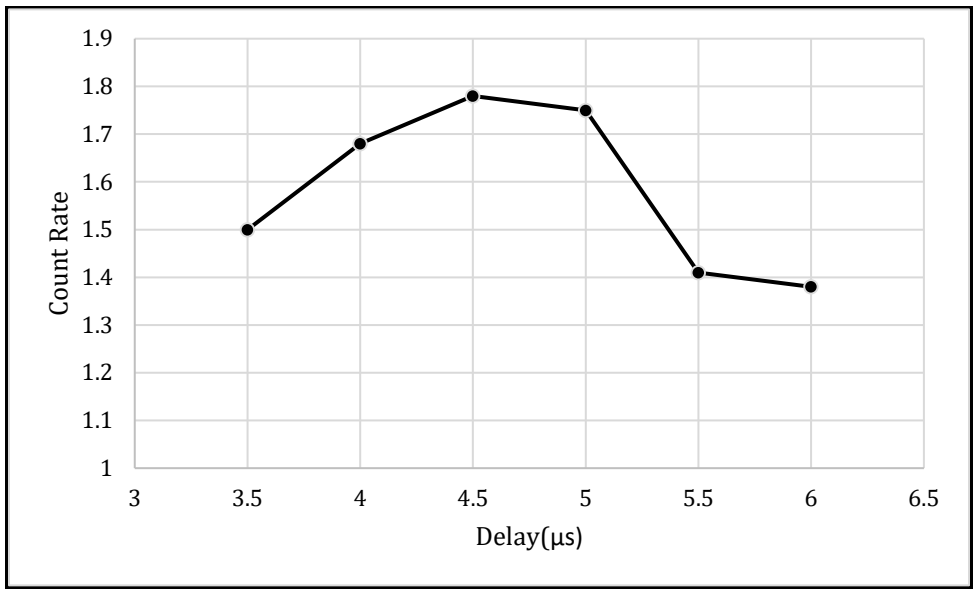

Figure 5.8 Count rate of the experimental setup as a function of Delay time set on the Gate and Delay Generator.

The plateau seen in Figure 5.8, represents the maximum counts per second where, the electron drift time matches the gate delay time of the surface barrier circuit. If the delay is set too high or too low, then the signal from the main GEM circuit won't coincide with the signal from the surface barrier detector circuit, and the count rate of the detector will drop as seen in Figure 5.8. The maximum counts per second for this setup was found to be 1.75 at a THGEM voltage of 550 and an induction voltage of 150V which agreed with the experimental results of Orchard *et al.* showing that the experimental set-up had been rebuilt successfully. The gain of the main amplifier used was 5x25. In order to determine the actual gain of the THGEM the gain of the preamplifier was required to be calculated as seen in the section below.

5.4.2 Determination of pre-amplifier gain

The THGEM placed in the EMS has a small induction gap between it and the anode. The anode of the EMS acquires the signal also known as the total charge collected and transmits it through a charge sensitive preamplifier before amplification by the main amplifier. Since the settings of the main amplifier are pre-set the only unknown is the gain of the pre-amplifier. The pre-amplifier designed by Canberra has an inbuilt gain that cannot be modified by the external circuit. The functionality of a pre-amplifier is to collect the charge obtained at the collection plate and convert it to a voltage pulse. This signal can then be transmitted to a main amplifier to be shaped and further amplified. In theory the gain of the preamplifier is constant throughout its operational history. In order to calculate its gain, the preamplifier was connected to an ORTEC 4000 pulse generator that sends out pre-set voltage pulses. The amplified pulse was viewed by an oscilloscope. The voltage pulse output on the oscilloscope had a peak which represented the gain of the preamplifier. The input voltage pulse was set at 200 mV which resulted in a 440 mV output from the oscilloscope. Hence, the gain was computed to be 2.2 as seen in the equation below.

$$G_{preamp} = \frac{V_{out}}{V_{in}} = \frac{440mV}{200mV} = 2.2 \qquad \text{(Equation 5.3)}$$

5.4.3 Experimental estimation of the THGEM Gain

The gain of the THGEM can be calculated by identifying the gain of the amplifier and preamplifier used in the circuit. The electrons created above the THGEM due to gas ionizations are driven down by a uniform electric field and multiplied by the THGEM to collect at the collection plate. The collection pad signal obtained is amplified by a preamplifier and furthermore by a main amplifier to obtain a peak using the multi-channel analyzer. By knowing the channel number to voltage conversion factor, the final signal

voltage can be calculated. This represents the total output of the system. In order to perform this experiment, a pulse generator was used initially with just the amplifier to identify the channel number to volts conversion factor.

As seen in Figure 5.9 the channel number to volts factors can be given by the solution of the line.

$$Total\ Output\ (V) = \frac{(Channel\#+\ 9)}{121.24} \qquad \text{(Equation 5.4)}$$

From this conversion factor the output signal in Volts can be converted to the number of electrons collected at the collection pad.

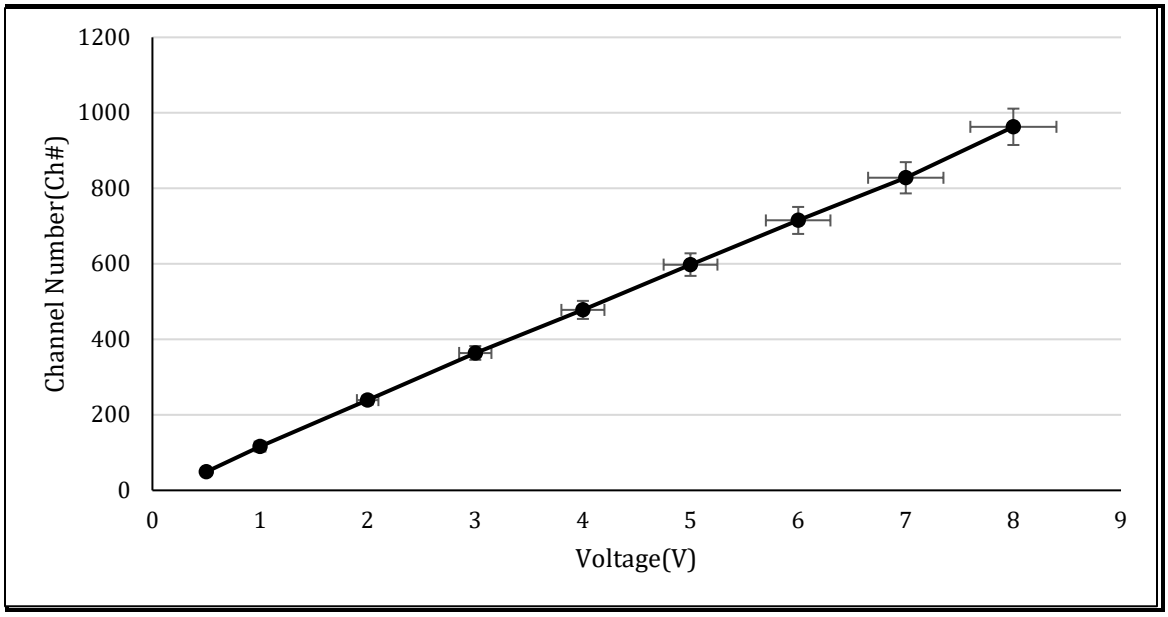

Figure 5.9 Channel number to voltage conversion factor.

The gain settings of the amplifier were set to a fine gain of 2.5 and a coarse gain of 40. The gain of the preamplifier was calculated to be 2.2. Finally, the sensitivity of the preamplifier was noted to be 235 mV/M ion pairs. With the above information the total output of the number of electrons collected is given by the following equation:

$$Number\ of\ Electrons\ Collected\ = \frac{V}{Gamp * Gpre-amp * S} \qquad \text{(Equation 5.5)}$$

The number of electrons generated in the drift chamber for the Am-241 source can be noted as $4.7*10^4$ on average as seen in a research study by Orchard *et al*. [45].Thus the absolute gain of the THGEM can be calculated as follows:

$$Absolute\ Gain(M) = \frac{Number\ of\ Electrons\ Collected}{Number\ of\ Electrons\ Generated} \qquad \text{(Equation 5.6)}$$

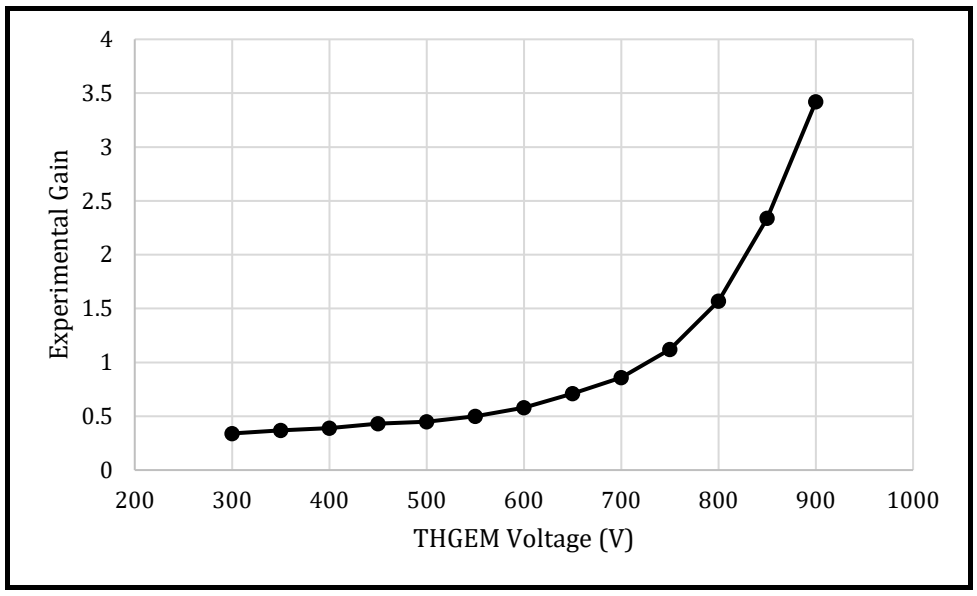

Figure 5.10 Experimental Gain vs THGEM voltage plot for the experimental setup.

As seen in Figure 5.10, the gain of the THGEM increases with the increase in the THGEM voltage. However, the gain measured is rather modest and the question arises as to whether a single GEM would be sufficient to measure tritium.

5.5 Comparison between Experimental and Simulation Gain

From the results obtained in the previous sections, the experimental and simulation gains were identified to be very similar trends to each other proving the efficacy of the

models. The gain in the simulation model increased with an increase in the THGEM voltage, starting with a very small increment at 600V and a more exponential increase after 700V. The magnitude of the changes in the experiment and the simulation showed very similar trends with an increase in the THGEM voltage. The introduction of penning transfers in the simulation code provided a greater increase in the gain's comparative to non-penning effects as seen in Figure 5.7. The Penning transfer effect was seen to be a very important component of the gain. This however cannot be accurately measured for every gas used in an experimental setup. From an experimental standpoint, the Penning transfer cannot be calculated and is assumed to be included in the gain results obtained. However, the variation between the experimental results and the simulation can be attributed to a lower Penning effect in the experiment or a slight presence of air in the experimental setup and possible ion back-flow leading to smaller electron avalanches and ultimately a lower gain. Figure 5.11 combines the data seen in Figures 5.7, and 5.10. The THGEM voltage in the experimental setup could not be pushed beyond 900 V due to the higher chance of breakdown and sparking.

However, as seen in Figure 5.11, the Penning gain is closely related to the experimental gain in trend at lower voltages. This shows that Penning effects exist in the experimental setup. The difference in magnitudes between the Penning and experimental gain suggest that the Penning transfer coefficient set for the simulation was overestimated. Furthermore, the experimental gain is seen to be higher than the Non-Penning gain initially as Penning effects are seen in the experimental setup. But after 850V the Non-Penning gain increases above the experimental gain for the same voltage. This can be explained by the fact that after 850V the experimental setup provided low resolution results as the THGEM

voltage maximum had been reached. Moreover, due to the presence of air in the setup and possible ion backflow as mentioned earlier, the experimental gain was reduced. A major difference in the gains between penning and non-penning cases signify the importance of penning transfer in the gain study using gas mixtures. Azevedo *et al.,* [52] observed a similar result where the penning played an important role in ensuring similarity between experiment and simulation. Thus, Penning effects should be considered when performing gain studies with any counting gas mixtures using simulation and modelling methods

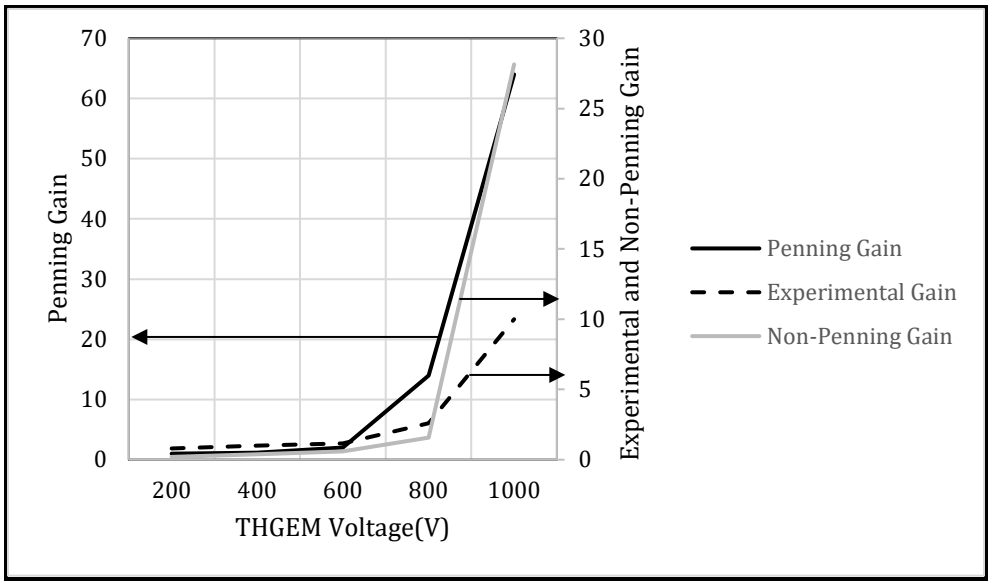

Figure 5.11 : Comparing the gain results obtained from experiment and simulation (Penning/Non-Penning).

5.6 Estimation of the uncertainty in experiment and simulation of THGEM gas gain

As mentioned earlier, the uncertainty of both experiment and simulation models must be calculated in order to increase the accuracy of the result. The simulation was performed for varying values of the THGEM voltage in order to see the dependence on gain. The result obtained for each run was the total number of electrons collected. As seen in Figures 5.1 and 5.2, a frequency distribution for 50 runs was plotted and the modal

number of electrons was chosen for calculations. In Figure 5.1, The modal number of electrons obtained was 455 for the highest frequency. Similarly, the modal number in Figure 5.2 for the tritium beta distribution was 450. Plots 5.1 and 5.2 were then converted to gain plots seen in Figures 5.3 and 5.4. As seen in Figure 5.3 most of the gain results lie between 2.01-2.15. This accounts for 68% of the total gain results. Using equation 4.1 the uncertainty can be calculated as 5.11%. Similarly, for Figure 5.4, most of the gain results lie between 1.95-2.10 which accounts for 62% of the total gain results. Using equation 4.1 the uncertainty in this case can be calculated as 6.4%.

Experimental uncertainty can be calculated as the individual uncertainties of the parameters involved. Since the experiment performed had a lot of components such as the pre-amplifier, amplifier, surface barrier detector etc., the uncertainty arises from each one of these components. A major source of uncertainty in the experiment is reading the result on the oscilloscope. The experimental uncertainty can be calculated as follows:

The experimental gain as seen in Equations can be written as:

$$Absolute\ Gain(M) = \frac{Number\ of\ Electrons\ Collected}{Number\ of\ Electrons\ Generated}$$

Where,

$$Number\ of\ Electrons\ Collected\ = \frac{V}{Gamp\ *\ Gpre-amp\ *\ S}$$

Pre-amplifier gain was observed to be 2.2. The preamplifier was connected to a pulser and the output pulse was viewed on the oscilloscope. The accuracy of each reading can be assumed to be 1/3rd of a division on the oscilloscope. For an input pulse of 200V $\pm$ 5% with an assumed uncertainty of 5% an output pulse of 440V was observed. This corresponds to 19 divisions on the oscilloscope scale. Therefore, the uncertainty for the

output pulse is 440 $\pm$ 2%. The total uncertainty for the pre-amp can be calculated as follows:

$$Gain = \frac{Output}{Input} = \frac{440 \ \pm 2\%}{200 \ \pm 5\%} = 2.2 \ \pm \sqrt{2^2 + 5^2} = 2.2 \pm 5.4\%$$

Similarly, the amplifier gain uncertainty was calculated to be 2%. The uncertainty in voltage comes from the voltage to channel number conversion seen in the following Equation.

$$Total\ Output\ (V) = \frac{(Channel\# + 9)}{121.24}$$

There are 1024 channels in the spectrum display. A 5% error can be assumed in reading the alpha peak from the spectrum display. The accuracy of each voltage reading on the oscilloscope was 1/3rd of a division. Thus, the uncertainty on the voltage can be calculated as 2%. The total uncertainty can be calculated as 5.4%.

The error in the number of electrons collected can be calculated as:

$$Number\ of\ Electrons\ Collected \ = \sqrt{5.4^2 + (5.4 + 2\ )^2} = \sqrt{84.3} = 9.18\%$$

Assuming the error on the number of electrons generated to be 5%, the total uncertainty of the experimental gain can be calculated to be 10.4%

5.7 Estimation of the number of THGEMs necessary for tritium detection

A single THGEM might not be enough to view tritium betas effectively due to its low gain obtained in both simulation and measurement. A multi-THGEM cascade, however, could be used in order to amplify the gains exponentially which will improve the efficiency of tritium detection. In order to estimate how many THGEMs will be necessary

the THGEM voltage is kept constant and using the gain obtained at that voltage, the calculation is performed for a single 5.68 keV beta particle.

For example, keeping the THGEM voltage constant at 850V, the gain of the THGEM is found to be 2.2 as seen in Figure 5.7.

A single 5.68 keV beta particle can produce approximately 220 electrons in P-10 gas, with a W-value of 26 eV/ion pair.

When multiplied, the total number of electrons collected at the collection plate is given as follows:

$$N_{tot} = \frac{5.6\ keV}{26\ eV} * 2.2 = 481 \qquad \text{(Equation 5.6)}$$

The electrons collected at the collection plate as the total output charge of the device will be converted to a voltage pulse by the preamplifier.

The sensitivity of the pre-amplifier = 235mV/M ion pair

And the Gain of the pre-amplifier = 2.2

Thus,

$$Voltage\ Pulse(V) = N_{tot} * 235\ mV * 10^{-6} * 2 = 225.6 * 10^{-6}\ V \qquad \text{(Equation 5.7)}$$

This voltage pulse is further amplified by a main amplifier with maximum gain settings.

Considering the maximum gain of the amplifier to be 40*10 = 400

The total voltage pulse obtained= $225.6 * 10^{-6}\ V * 400 = 90240 * 10^{-6}\ V = 0.09V$

The multichannel analyzer software consists of 1024 channels. Using the voltage pulse to channel number approximation seen in Equation 5.4, the channel number for a single tritium beta can be obtained.

$$Channel\# = (Total\ Output\ V * 121.24) - 9 \qquad \text{(Equation 5.8)}$$

Thus,

$$Channel\# = (0.09 * 121.24) - 9 = 2 \quad \text{(Equation 5.10)}$$

The beta particle releasing 220 electrons multiplied using a THGEM will show at channel# 2 at the multi-channel analyzer software. This will make it indistinguishable from the noise that is present in the circuit. A solution to this issue would be to add multiple THGEMs in a cascade to increase the gain and clearly define the signal.

Considering the THGEM cascade has 3 THGEMs, the total gain of the system will be 2.2*2.2*2.2 = 10.6

Using the same conditions as above, the total number of electrons collected at the collection plate for a single beta event will be:

$$N_{tot} = 10.6 * 220 = 2332\ electrons \quad \text{(Equation 5.11)}$$

The new voltage pulse at the pre-amplifier will be:

$$Voltage\ Pulse\ (V) = N_{tot} * 235\ mV * 10^{-6} ion\ pairs * 2 = 1096 * 10^{-6}\ V$$

Which implies,

$$1096 * 10^{-6}\ V * 400 = 438400 * 10^{-6}\ V = 0.4V$$

Converting this to a Channel # would result in:

$$Channel\ \# = (0.4 * 121.24) - 9 = 40$$

This would make the signal visible in the software against the noise and the background radiation. Thus, a single THGEM is not enough to view a signal from a beta event. However, a THGEM cascade with 3-4 THGEMs will be able to produce enough charge at the collection plate to increase the signal strength and detection efficiency.

Chapter 6 Conclusion and Future Work

Tritium is widely known to be a by-product of CANDU nuclear reactors that use heavy water for their moderator and coolants. The increase in the production of tritium has led to active research in tritium detection and dosimetry due to its detrimental effects on humans and the environment. Tritium however is a low energy beta emitter with an average energy of 5.68 keV. With the advancement in technical standards in the nuclear industry, various new techniques have been considered for tritium detection. Gas electron multipliers investigated in this thesis is one such promising detection methods. This thesis investigated the efficiency of Thick-GEMS for the detection of tritium. The results of this investigation showed that the THGEM gain was found to be low, showing a meagre 0.5 for 600V and 2.2 at 850V in the experiment and 20.5 in the simulation with penning transfer for the same conditions as seen in Figure 5.11. The optimum collection pad size was found to be 2.2-2.5 mm at a drift length of 0.1 cm. From the results obtained the following general conclusions can be drawn:

- The optimum collection pad size was found to be 2.5 mm x 2.5 mm for a single tritium beta particle using a THGEM at a drift length of 0.1 mm and a drift field of 274 V/cm. The pad size depends on various factors including the drift length and the drift electric field that must be taken into consideration for its design. Further research should be performed with the data obtained in this thesis to develop a model of a tritium detector with multiple pads of a pad size appropriate to the set conditions of drift length and drift field in order to differentiate tritium from other radiation types with a pad triggering mechanism based on the distance travelled in the gas.

- Single THGEMs have a modest gain for the operating voltages they can tolerate before sparking. The gains obtained both experimentally and through simulation models do not seem to be sufficient for tritium detection. However, multi-level cascades with 3 or more THGEMS should prove to have enough gain to detect tritium. Since THGEMs are very easily mass produced in comparison to their thin counterparts, more research must be performed on the THGEM cascades with simulation and experimental models to be used for tritium detection.
- Gain depends on the voltage of the THGEM and the possibility of Penning transfers within the gas used. For this thesis, a Penning transfer of 19 percent was used in order to calculate the gains in the simulation model. The Penning effect must be researched further with other gas mixtures from a simulation standpoint to investigate which gas is ideal for tritium detection.
- Unlike THGEMs, Thin-GEMS have also been widely used in radiation detectors in the nuclear industry. Thin-GEMs must be further investigated to prove its efficacy over THGEM in terms of gain. Thin-GEMs are thinner and hence show a greater electric field strength at the holes. This in turn increases the multiplication factor of the GEM. Moreover, the trapezoidal hole design versus a cylindrical hole design is known to confine the interactions in a tighter space thereby increasing the gain of the system.

The long-term aim of this thesis is the design of an optimized tritium detector that can not only detect tritium more efficiently, but also be able to differentiate it from other types of radiation in a mixed field environment. The ideal collection pad size allows the designer to consider the possibility of having multiple pads that trigger based on the distance travelled

by the beta particle of electron in the gas. In this hypothetical scenario, tritium would trigger only 1 or two pads versus a long-range beta particle which would trigger more than 2 pads. Thin and Thick GEMs must be compared in terms of the raw gain and further studied to provide information about discharges and the maximum voltage that can be achieved without failure.

References

[1] N. R. Council, D. on E. and L. Studies, and C. on G. Resources Environment and, *Research Needs in Subsurface Science*. National Academies Press, 2000.

[2] S. Dingwall, C. E. Mills, N. Phan, K. Taylor, and D. R. Boreham, "Human Health and the Biological Effects of Tritium in Drinking Water: Prudent Policy Through Science – Addressing the ODWAC New Recommendation," *Dose-Response*, vol. 9, no. 1, pp. 6–31, Feb. 2011.

[3] H. A. Schmutz, P. Sabharwall, and C. Stoots, "Tritium Formation and Mitigation in High- Temperature Reactors," p. 33, U.S, N.p, Oct. 2012.

[4] Canadian Nuclear Safety Commission, *Tritium releases and dose consequences in Canada in 2006: Part of the Tritium studies project.* Ottawa, Ontario: Canadian Nuclear Safety Commission, 2009.

[5] D. I. Fairlie., "*Tritium Hazard Report: Pollution and Radiation Risk from Canadian Nuclear Facilities*," p. 92. Green Peace Canada, 2007

[6] N. R. Council, *Safety and Security of Commercial Spent Nuclear Fuel Storage: Public Report*. 2005.

[7] OECD and Nuclear Energy Agency, *The Safety of the Nuclear Fuel Cycle - Third Edition*. OECD, 2005.

[8] M. Buckthought, "Tritium on Tap: Keep radioactive tritium out of our drinking water," p. 50., Sierra Club Canada, 2009

[9] J. R. Parrington, H. D. Knox, S. L. Breneman, and E. M. F. Baum, "Nuclides and isotopes: Wall chart information booklet. Fifteenth edition, revised 1996," Knolls Atomic Power Lab., Schenectady, NY (United States); General Electric Co., San Jose, CA (United States). Nuclear Energy Div., GE-97001961, Dec. 1996.

[10] L. I. Bodine, D. S. Parno, and R. G. H. Robertson, "Assessment of molecular effects on neutrino mass measurements from tritium beta decay," *Phys. Rev. C*, vol. 91, no. 3, p. 035505, Mar. 2015.

[11] R. J. Budnitz, "Tritium Instrumentation for Environmental and Occupational Monitoring - A Review:" *Health Phys.*, vol. 26, no. 2, pp. 165–178, Feb. 1974.

[12] J. D. Harrison, A. Khursheed, and B. E. Lambert, "Uncertainties in dose coefficients for intakes of tritiated water and organically bound forms of tritium by members of the public," *Radiat. Prot. Dosimetry*, vol. 98, no. 3, pp. 299–311, 2002.

[13] S. Diabaté and S. Strack, “Organically bound tritium.,” *Health Phys.*, vol. 65, no. 6, pp. 698–712, Dec. 1993.

[14] R. L. Dobson, “The toxicity of tritium,” *Biol. Implic. Radionucl. Released Nucl. Ind.*, National Technical Information Service 1979.

[15] J. W. Laskey and S. J. Bursian, “Some effects of chronic tritium exposure during selected ages in the rat,” *Radiat. Res.*, vol. 67, no. 2, pp. 314–323, Aug. 1976.

[16] G. V. Last *et al.*, “Vadose Zone Hydrogeology Data Package for Hanford Assessments,” PNNL-14702 Rev. 1, 896355, Jun. 2006.

[17] P.Ting and M. K. Sullivan, "Reactor Coolant Monitoring with a Discrete Sampling Flow Cell Scintillator System", Sixteenth Annual Meeting of the Health Physics Society, 1971

[18] R. A. Surette and R. G. C. McElroy, “A REVIEW OF TRITIUM-IN-WATER MONITORS,” p. 13, 1986.

[19] C. J. Huntzinger *et. al*, "A Real-Time Monitor for Tritium in Waste Water", Hazards Control Department Annual Technology Review, LLNL, UCRL-50007-82,1983

[20] C. D. R. Azevedo *et al.*, “TRITIUM - A Real-Time Tritium Monitor System for Water Quality Surveillance,” *ArXiv190205456 Phys.*, Feb. 2019.

[21] T. Uda *et.al*,“Detection efficiency of plastic scintillator for gaseous tritium sampling and measurement system", Fusion Engineer and Design, Elsivier, Vol. 85(7-9),pp. 1474-1478, Dec. 2010

[22] A. Kumar and A. J. Waker, “An experimental study of the relative response of plastic scintillators to photons and beta particles,” *Radiat. Meas.*, vol. 47, no. 10, pp. 930–935, Oct. 2012.

[23] W.L. Marter and C. M. Patterson, “Monitoring of Tritium in Gases, Liquids, and in the Environment", Trans. Am. nucl. Soc., 14:1, pp. 162-163. June. 1971

[24] Sartex Power Control Systems Inc., “Portable-Tritium-in-Air-Monitor-Model-209L-Sartrex". [Online]. Available: http://sartrex.ca/solutions-overview/health-physics-products/portable-tritium-in-air-monitor-model-209l. [Accessed: 25-Sept-2019]

[25] S. N. Ahmed, “11 - Dosimetry and radiation protection,” in *Physics and Engineering of Radiation Detection (Second Edition)*, Ed. Elsevier, 2015, pp. 621–688.

[26] F. Sauli, “The gas electron multiplier (GEM): Operating principles and applications,” *Nucl. Instrum. Methods Phys. Res. Sect. Accel. Spectrometers Detect. Assoc. Equip.*, vol. 805, pp. 2–24, Jan. 2016.

[27] G. Charpak and F. Sauli, “The multistep avalanche chamber: A new high-rate, high-accuracy gaseous detector,” *Phys. Lett. B*, vol. 78, no. 4, pp. 523–528, Oct. 1978.

[28] F. Sauli, “GEM: A new concept for electron amplification in gas detectors,” *Nucl. Instrum. Methods Phys. Res. Sect. Accel. Spectrometers Detect. Assoc. Equip.*, vol. 386, no. 2, pp. 531–534, Feb. 1997.

[29] A. Bondar, A. Buzulutskov, A. Grebenuk, D. Pavlyuchenko, Y. Tikhonov, and A. Breskin, “Thick GEM versus thin GEM in two-phase argon avalanche detectors,” *J. Instrum.*, vol. 3, no. 07, pp. P07001–P07001, Jul. 2008.

[30] A. Sipaj., “Simulation, design and construction of a gas electron multiplier for particle tracking,” M.A.S.c Thesis, Ontario Tech University, ON, Canada, Dec. 2012.

[31] X.-F. Navick *et al.*, “Fabrication of ultra-low radioactivity detector holders for Edelweiss-II,” *Nucl. Instrum. Methods Phys. Res. Sect. Accel. Spectrometers Detect. Assoc. Equip.*, vol. 520, no. 1, pp. 189–192, Mar. 2004.

[32] G. M. Orchard, S. Puddu, and A. J. Waker, “Design and function of an electron mobility spectrometer with a thick gas electron multiplier,” *Nucl. Instrum. Methods Phys. Res. Sect. Accel. Spectrometers Detect. Assoc. Equip.*, vol. 815, pp. 62–67, Apr. 2016.

[33] R. Chechik *et. al,* “Thick GEM-like (THGEM) Detectors and Their Possible Applications,” SNIC Symp. Stanf. Calif. USA, p. 3, Apr. 2006.

[34] J. E. Turner, “Interaction of ionizing radiation with matter”, Health Physics, vol. 86(3),pp. 228-252, Mar. 2004

[35] G. F. Knoll, *Radiation Detection and Measurement*. John Wiley & Sons, 2010.

[36] J. Seco and F. Verhaegen, “Monte Carlo Techniques in Radiation Therapy,” *CRC Press*. [Online]. Available: https://www.crcpress.com/Monte-Carlo-Techniques-in-Radiation-Therapy/Seco-Verhaegen/p/book/9781138199903. [Accessed: 16-Jul-2019].

[37] R. Morin, "*Monte Carlo Simulation in the Radiological Sciences*.",CRC Press.[Online].Available: https://pubs.rsna.org/doi/abs/10.1148/radiology.173.1.36?journalCode=radiology. [Accessed: 16-Jul-2019].

[38] S. Agostinelli *et al.*, “GEANT4-a simulation toolkit,” *Nucl. Instrum. Methods Phys. Res. Sect. Accel. Spectrometers Detect. Assoc. Equip.*, vol. 506, p. 250, Jul. 2003.

[39] J. Allison *et al.*, “Recent developments in Geant4,” *Nucl. Instrum. Methods Phys. Res. Sect. Accel. Spectrometers Detect. Assoc. Equip.*, vol. 835, pp. 186–225, Nov. 2016.

[40] P. Arce, P. Rato, M. Canadas, and J. I. Lagares, “GAMOS: A Geant4-based easy and flexible framework for nuclear medicine applications,” in *2008 IEEE Nuclear Science Symposium Conference Record*, 2008, pp. 3162–3168.

[41] A. K. Glaser, S. C. Kanick, R. Zhang, P. Arce, and B. W. Pogue, “A GAMOS plug-in for GEANT4 based Monte Carlo simulation of radiation-induced light transport in biological media,” *Biomed. Opt. Express*, vol. 4, no. 5, pp. 741–759, May 2013.

[42] H.Schindler and R. Veenhof ,“Garfield++ – simulation of ionisation based tracking detectors.” [Online]. Available: http://garfieldpp.web.cern.ch/garfieldpp/. [Accessed: 21-Jul-2019].

[43] C.Geuzaine and J. F. Remacle,“Gmsh: a three-dimensional finite element mesh generator with built-in pre- and post-processing facilities.” [Online]. Available: http://gmsh.info/. [Accessed: 21-Jul-2019].

[44] P. Ponomarev, "*SEMTEC Report Elmer FEM - Induction Machine Tutorial*.", VTT Technical Research Centre of Finland Ltd, Research Report, Espoo, Finland, May 2017. Available at: https://doi.org/10.12140/RG.2.2.18599.75688J

[45] G. M. Orchard and A. J. Waker, “Transit time of electrons and gas gain effects in P-10 and Ar+CO2,” *Nucl. Instrum. Methods Phys. Res. Sect. Accel. Spectrometers Detect. Assoc. Equip.*, vol. 764, pp. 236–240, Nov. 2014.

[46] R. A. Surette and J. Dubeau, “Tritium discrimination using cluster size information from a DGEM detector,” *Nucl. Instrum. Methods Phys. Res. Sect. Accel. Spectrometers Detect. Assoc. Equip.*, vol. 539, no. 1, pp. 433–440, Feb. 2005.

[47] R. Chechik, A. Breskin, and C. Shalem, “Thick GEM-like multipliers—a simple solution for large area UV-RICH detectors,” *Nucl. Instrum. Methods Phys. Res. Sect. Accel. Spectrometers Detect. Assoc. Equip.*, vol. 553, no. 1, pp. 35–40, Nov. 2005.

[48] A. Breskin *et al.*, “A concise review on THGEM detectors,” *Nucl. Instrum. Methods Phys. Res. Sect. Accel. Spectrometers Detect. Assoc. Equip.*, vol. 598, no. 1, pp. 107–111, Jan. 2009.

[49] A. Brodsky, “The Stochastic Nature of All Radiation Effects,” *Health Phys.*, vol. 102, no. 3, p. 348, Mar. 2012.

[50] J. R. DeVore and M. A. Buckner, “Tritium monitoring techniques,” ORNL/TM--13132, 236278, May 1996.

[51] Ö. Şahin, I. Tapan, E. N. Özmutlu, and R. Veenhof, "Penning transfer in argon-based gas mixtures," *J. Instrum.*, vol. 5, no. 05, pp. P05002–P05002, May 2010.

[52] C. D. R. Azevedo, P. M. Correia, L. F. N. D. Carramate, A. L. M. Silva, and J. F. C. A. Veloso, "THGEM gain calculations using Garfield++: Solving discrepancies between the simulation and experimental data," *J. Instrum.*, vol. 11, no. 08, pp. P08018–P08018, Aug. 2016.

Appendix A. A Sample Geant 4/GAMOS Simulation Code

The following code is a macro used by GAMOS to simulate a 5.68 keV mono energetic electron point source in a simple geometry to calculate the ionization cluster size.

```
//Setting parameters and geometry from test.geom
/tracking/verbose 1
/gamos/setParam GmGeometryFromText:FileName test.geom
/gamos/geometry GmGeometryFromText
/gamos/physicsList GmEMExtendedPhysics
#/gamos/GmPhysics/replacePhysics electron-lowener
/gamos/generator GmGenerator
//Initializes the geometry and runs the commands
/run/initialize
//Setting up the source properties with position, direction with respect to the geometry and energy
/gamos/generator/addSingleParticleSource source H3 5.68*keV
/gamos/generator/directionDist source GmGenerDistDirectionRandom
/gamos/generator/positionDist source GmGenerDistPositionPoint 0. 0. 0.
//Counter for tracks
/gamos/userAction GmCountProcessesUA
//Initializes VRML 2 and OGLIX viewers
/control/execute /home/gamos/gamos/GAMOS.5.1.0/examples/visVRML2FILE.in
/control/execute ../visOGLIX.in
/gamos/userAction GmTrackDataHistosUA
//Number of events
/run/beamOn 50
```

Appendix B. A Sample Garfield++ Code

```
//This code simulates the THGEM geometry and the electron avalanche process. The base
code was obtained from the Garfield++ website [40] and modified to suit the thesis
objectives.

#include <iostream>
#include <cmath>

#include <TCanvas.h>
#include <TApplication.h>
#include <TFile.h>

#include "MediumMagboltz.hh"
#include "ComponentElmer.hh"
#include "Sensor.hh"
#include "ViewField.hh"
#include "Plotting.hh"
#include "ViewFEMesh.hh"
#include "ViewSignal.hh"
#include "GarfieldConstants.hh"
#include "Random.hh"
#include "AvalancheMicroscopic.hh"

using namespace Garfield;

int main(int argc, char* argv[]) {

  TApplication app("app", &argc, argv);

  // Set THGEM parameters
  // THGEM thickness in cm
  const double gem_th = 0.012;
  // Copper plate thickness
  const double gem_cpth = 0.005;
  // THGEM pitch
  const double gem_pitch = 0.08;
  // X-width of drift simulation(+/-)
  const double axis_x = 0.1;
  // Y-width of drift simulation(+/-)
  const double axis_y = 0.1;
  // Initial position of particle above the THGEM
  const double axis_z = 0.25 + gem_th / 2 + gem_cpth;


  // Calls the Magboltz program to initialize properties of the drift medium
  MediumMagboltz* gas = new MediumMagboltz();
  // Set the temperature (K)
  gas->SetTemperature(293.15);
  // Set the pressure (Torr)
  gas->SetPressure(760.);
  // Enables drift in the medium
  gas->EnableDrift();
  // Specify the gas mixture (Ar/CH4 90:10)
  gas->SetComposition("ar", 90., "ch4", 5.);

//Ion mobility file for Ar gas to assist in the drift calculation
const std::string path = getenv("GARFIELD_HOME");
  gas->LoadIonMobility(path + "/Data/IonMobility_Ar+_Ar.txt");
```

```
// Setting penning coefficient for the simulation at 0.19 or 19%
  const double rPenning = 0.19;
  const double lambdaPenning = 0.;
  gas->EnablePenningTransfer(rPenning, lambdaPenning, "ar");

  // Imports electric field map for the THGEM geometry from ELMER
  ComponentElmer* elm = new ComponentElmer(
      "gemcell/mesh.header", "gemcell/mesh.elements", "gemcell/mesh.nodes",
      "gemcell/dielectrics.dat", "gemcell/gemcell.result", "cm");
  elm->EnablePeriodicityX();
  elm->EnableMirrorPeriodicityY();
  elm->SetMedium(0, gas);

  // Sets up a sensor object for visualization
  Sensor* sensor = new Sensor();
  sensor->AddComponent(elm);
  sensor->SetArea(-axis_x, -axis_y, -axis_z, axis_x, axis_y, axis_z);

  // Module to simulate avalanches in the geometery
  AvalancheMicroscopic* aval = new AvalancheMicroscopic();
  aval->SetSensor(sensor);
  aval->SetCollisionSteps(100);


  // object for drift line visualization.
  ViewDrift* viewDrift = new ViewDrift();
  viewDrift->SetArea(-axis_x, -axis_y, -axis_z, axis_x, axis_y, axis_z);
  aval->EnablePlotting(viewDrift);

  // Set the electron start parameters.
  // Staring arbitrary position of electron above the THGEM
  const double zi = 0.25 * gem_th/2 + gem_cpth;
  double ri = (gem_pitch / 2) * RndmUniform();
  double thetai = RndmUniform() * TwoPi;
  double xi = ri * cos(thetai);
  double yi = ri * sin(thetai);
  double ti = 0.;

  // Module for tritium energy distribution using selection algorithm based on
probability of occurrence
  double ei = 0;
  float val=(double)rand()/RAND_MAX;
  if(val<0.190845)
  ei=rand()%2000;
  else if(val<0.394769)
  ei=rand()%2001 + 2000;
  else if(val<0.57987721)
  ei=rand()%2001 + 4000;
  else if(val<0.73281071)
  ei=rand()%2001 + 6000;
  else if(val<0.84888683)
  ei=rand()%2001 + 8000;
  else if(val<0.92800905)
  ei=rand()%2001 + 10000;
  else if(val<0.97431205)
  ei=rand()%2001 + 12000;
  else if(val<0.995219)
```

```
ei=rand()%2001 + 14000;
else if(val<0.99991)
ei=rand()%2001 + 16000;
else
ei=rand()%1001 + 18000;

// Calculate the avalanche and get electron end points
aval->AvalancheElectron(xi, yi, zi, ti, ei, 0., 0., 0.);
std::cout << "... avalanche complete with "
          << aval->GetNumberOfElectronEndpoints() << " electron tracks.\n";


// Write the histograms to the TFile.
hS->Write();
hInt->Write();
f->Close();

// Plot the geometry, field and drift lines.
TCanvas* cGeom = new TCanvas("geom", "Geometry/Avalanche/Fields");
cGeom->SetLeftMargin(0.14);
const bool plotContours = false;
if (plotContours) {
  ViewField* vf = new ViewField();
  vf->SetSensor(sensor);
  vf->SetCanvas(cGeom);
  vf->SetArea(-axis_x, -axis_y, axis_x, axis_y);
  vf->SetNumberOfContours(40);
  vf->SetNumberOfSamples2d(30, 30);
  vf->SetPlane(0, -1, 0, 0, 0, 0);
  vf->PlotContour("v");
}

}

app.Run(kTRUE);
 return 0;}
```